

# Superconducting Orbital Magnetoelectric Effect and the Case Study of Twisted Bilayer Graphene

Wen-Yu He<sup>1,\*</sup> and K. T. Law<sup>2,†</sup>

<sup>1</sup>*Department of Physics, Massachusetts Institute of Technology, Cambridge, Massachusetts 02139, USA*

<sup>2</sup>*Department of Physics, Hong Kong University of Science and Technology, Clear Water Bay, Hong Kong, China*

(Dated: June 22, 2022)

In noncentrosymmetric superconductors, previous studies on the supercurrent-induced magnetization mainly focused on the spin magnetization related to spin-orbit coupling (called the spin magnetoelectric effect or the Edelstein effect). However, the Berry curvature effects of the normal state band structure is ignored. In this work, we show that Berry curvatures in superconductors can induce large orbital magnetization in the presence of a supercurrent. We constructed a unified description for the current-induced spin and orbital magnetization effect across the superconductivity-normal metal phase transition. We find that in a superconductor with uniform pairing, the current-induced magnetization at a given current density is the same as that in its normal metal phase, while with the nonuniform superconducting pairing, the current-induced magnetization can have an abrupt change in magnitude near the superconductor-normal metal phase transition. Importantly, our theory predicts the orbital magnetoelectric effect in superconducting twisted bilayer graphene which has paired Bloch electrons with large orbital magnetic moments and negligible spin-orbit coupling. We propose that measurement of the current-induced orbital magnetoelectric effect can be used to detect the possible non-uniform pairings in twisted-bilayer graphene and other newly discovered superconductors with non-trivial Berry curvatures.

*Introduction.*— Noncentrosymmetric superconductors with spin-orbit coupling (SOC) can have supercurrent-induced spin magnetization, which is known as the superconducting spin magnetoelectric effect (or the Edelstein effect) [1, 1–6]. The SOC, which couples the spin magnetic moment of a Bloch electron with its crystal momentum, can endow moving Cooper pairs with net spin polarization [8], so the spin magnetoelectric effect in noncentrosymmetric superconductors arises from the SOC. In addition to the SOC, inversion symmetry breaking can give rise to nonzero Berry curvature to Bloch electrons [9]. The Bloch electrons with nonzero Berry curvature are self-rotating and carry finite orbital magnetic moments [9–11]. In a crystal, the orbital magnetic moment together with the spin magnetic moment compose the total intrinsic magnetic moment of a Bloch electron [9–15].

In a normal metal of gyrotropic point group symmetry [16, 17], applying a current induces a magnetic moment distribution imbalance on the Fermi surfaces and generates both spin [18, 19] and orbital magnetization [2, 21]. While the supercurrent induced spin magnetization has been studied extensively in previous works [1, 1–6, 16], the Berry curvature effect on the supercurrent induced magnetization has been ignored. Thus, it has not been clear if Cooper pairs formed by electrons with orbital magnetic moments can cause net orbital magnetization in the presence of a supercurrent. In this work, we take into account the orbital magnetic moments carried by Bloch electrons and show that applying supercurrent can generate orbital magnetization. Moreover, we constructed a unified description for the current-induced magnetization that is applicable in both the su-

perconductivity and the normal metal region. We note that, with uniform  $\mathbf{k}$ -independent pairing (such as s-wave pairing), the current-induced magnetization remains the same across the critical temperature  $T_c$ , given the same current density. However, for  $\mathbf{k}$ -dependent pairing, there is a jump in magnitude of the magnetization across  $T_c$ . Therefore, measurement of the current-induced magnetization effect provides a new way to detect unconventional superconductivity.

Importantly, our theory can be applied to twisted bilayer graphene (TBG) which has large Berry curvature and negligible SOC. TBG has recently been observed to exhibit both superconductivity [22–27] and orbital magnetism [25, 28–31]. When TBG is coupled to a hexagonal boron nitride (hBN) substrate, the alignment of TBG with hBN breaks the sublattice symmetry in the bottom layer graphene and creates finite Berry curvature in the Moiré flat bands [6, 33–35]. Due to the nonzero Berry curvature, the strong electronic correlations in TBG can result in a quantum anomalous Hall state with net orbital magnetization [6, 25, 28–31, 33–35] and current-induced magnetization switching [28, 29, 36]. Importantly, the superconductivity and orbital magnetism have been observed in the same TBG sample (at different filling factors) [25], indicating that the Cooper pairs can be formed by electrons carrying finite orbital magnetic moments. In this work, we predict that TBG exhibits supercurrent induced orbital magnetization (or the orbital magnetoelectric effect) even though SOC is negligibly small. Importantly, we further point out that the measurement of the orbital magnetization can test whether superconducting TBG has uniform or non-uniform pairing order parameters. Besides being applicable to TBG, our theory is

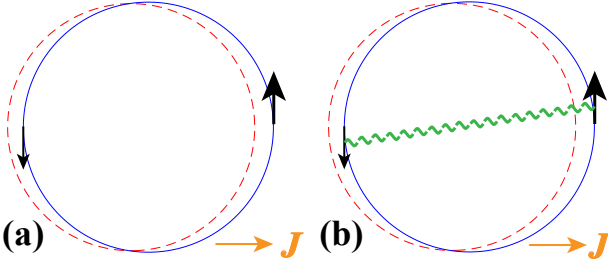


FIG. 1: The perturbation of applying current to a normal metal (a) and a superconductor (b). The blue and red circle correspond to the Fermi surface with and without current respectively. In a normal metal, applying current makes more electronic states with net momentum parallel to the applied current density  $\mathbf{J}$  occupied at the Fermi energy. Correspondingly, net magnetization can arise from the magnetic moments in the Bloch electrons. In a superconductor, the Bloch electrons of net momentum get paired to form Cooper pairs of net momentum. The magnetic moments carried by the paired Bloch electrons are involved in the pairing condensation and can generate a net magnetization. The black arrow denotes the total magnetic moment carried by the electrons moving forward or backward, and the amplitude is schematically represented by the size of the arrow.

generally applicable to a large number of noncentrosymmetric superconductors with finite Berry curvatures.

*A unified description for the magnetoelectric effect.*— In a noncentrosymmetric crystal, both the normal and superconducting states can be described by the Bogliubov-de Gennes Hamiltonian

$$\mathcal{H} = \frac{1}{2} \sum_{\mathbf{k}} \begin{pmatrix} c_{\mathbf{k}}^{\dagger} & c_{-\mathbf{k}} \end{pmatrix} \begin{pmatrix} H_0(\mathbf{k}) & \hat{\Delta}(\mathbf{k}) \\ \hat{\Delta}^{\dagger}(\mathbf{k}) & -H_0^*(-\mathbf{k}) \end{pmatrix} \begin{pmatrix} c_{\mathbf{k}} \\ c_{-\mathbf{k}}^{\dagger} \end{pmatrix}, \quad (1)$$

with  $H_0(\mathbf{k})$  being the normal state Hamiltonian matrix,  $\hat{\Delta}(\mathbf{k})$  the pairing matrix and  $c_{\mathbf{k}}^{\dagger}(c_{\mathbf{k}})$  the creation (annihilation) operator that includes multiple components for all the orbital and spin degrees of the system. In the normal state, a Bloch electronic state  $|\phi_{\nu,\mathbf{k}}\rangle$  with energy  $\xi_{\nu,\mathbf{k}} = \langle \phi_{\nu,\mathbf{k}} | H_0(\mathbf{k}) | \phi_{\nu,\mathbf{k}} \rangle$  carries the spin magnetic moment  $\mathbf{S}_{\nu,\mathbf{k}} = \langle \phi_{\nu,\mathbf{k}} | \frac{1}{2} \mu_B g \boldsymbol{\sigma} | \phi_{\nu,\mathbf{k}} \rangle$ , with  $\mu_B$  being the Bohr magneton and  $g$  the Lande  $g$  factor. In the absence of inversion symmetry, nonzero Berry curvature  $\boldsymbol{\Omega}_{\nu,\mathbf{k}} = i \langle \partial_{\mathbf{k}} \phi_{\nu,\mathbf{k}} | \times | \partial_{\mathbf{k}} \phi_{\nu,\mathbf{k}} \rangle$  can arise and endow the Bloch electronic state with finite orbital magnetic moment  $\mathbf{m}_{\nu,\mathbf{k}} = \frac{ie}{2\hbar} \langle \partial_{\mathbf{k}} \phi_{\nu,\mathbf{k}} | \times [H_0(\mathbf{k}) - \xi_{\nu,\mathbf{k}}] | \partial_{\mathbf{k}} \phi_{\nu,\mathbf{k}} \rangle$  [9–11]. Therefore, the total magnetic moment of a Bloch electron is  $\mathbf{M}_{\nu,\mathbf{k}} = \mathbf{S}_{\nu,\mathbf{k}} + \mathbf{m}_{\nu,\mathbf{k}}$ . In the superconduct-

ing state with time reversal symmetry, as a Bloch electronic state  $|\phi_{\nu,\mathbf{k}}\rangle$  always has a partner  $|\phi_{\nu,-\mathbf{k}}\rangle$  with the same energy  $\xi_{\nu,\mathbf{k}} = \xi_{\nu,-\mathbf{k}}$ , the two Bloch electronic states can pair and give rise to the pairing order parameter  $\Delta_{\nu,\mathbf{k}} \sim \langle \phi_{\nu,-\mathbf{k}} \phi_{\nu,\mathbf{k}} \rangle$  [37, 38], yielding the Bogliubov quasiparticle spectrum  $\epsilon_{\nu,\mathbf{k}} = \sqrt{\xi_{\nu,\mathbf{k}}^2 + |\Delta_{\nu,\mathbf{k}}|^2}$ . Therefore, in a superconductor with finite Berry curvature, the paired electrons generally carry both spin and orbital magnetic moments even though the net magnetization is zero in the absence of a current. However, as we show below, a current can induce net spin and orbital magnetization.

In a superconductor, applying a current can be described by introducing a  $U(1)$  gauge field to the original Hamiltonian  $\mathcal{H} \rightarrow \mathcal{H} + \delta\mathcal{H}$  where

$$\delta\mathcal{H} = - \sum_{\mathbf{k},\mathbf{q}} c_{\mathbf{k}-\frac{1}{2}\mathbf{q}}^{\dagger} c_{\mathbf{k}+\frac{1}{2}\mathbf{q}} \left[ \frac{e}{\hbar} \partial_{k_i} H_0(\mathbf{k}) A_i(-\mathbf{q},t) - \frac{e^2}{2\hbar^2} \partial_{k_i k_j}^2 H_0(\mathbf{k}) A_i(\mathbf{q},t) A_j(-\mathbf{q},t) \right], \quad (2)$$

with the spatial components denoted by  $i, j = x, y, z$ , and  $\mathbf{A}(\mathbf{r},t) = \sum_{\mathbf{q}} \mathbf{A}(\mathbf{q},t) e^{i\mathbf{q}\cdot\mathbf{r}}$ , the vector gauge potential. The perturbation  $\delta\mathcal{H}$  changes the distribution of Bloch electrons at the Fermi energy and also changes the original Fermi surfaces, as is schematically shown in Fig. 1 (a). In the normal metallic state, the redistribution of Bloch electrons results in an imbalance of the total magnetic moments of the occupied states, and a net magnetization arises by applying a current. In the superconducting state, the supercurrent is proportional to  $\sum_{\mathbf{q}} \mathbf{q} \Delta_{\nu,\mathbf{k},\mathbf{q}}^* \Delta_{\nu,\mathbf{k},\mathbf{q}}$  with  $\Delta_{\nu,\mathbf{k},\mathbf{q}} \sim \langle \phi_{\nu,-\mathbf{k}+\frac{1}{2}\mathbf{q}} \phi_{\nu,\mathbf{k}+\frac{1}{2}\mathbf{q}} \rangle$ , where  $\mathbf{q}$  is the net momentum of a Cooper pair. As a result, the supercurrent induces a net magnetic moment which involves both the spin and orbital components in the paired Bloch electronic states. Interestingly, the way for supercurrent to induce net magnetization is in analogy to that in the normal metallic state: in the superconductivity case the supercurrent accumulates net spin and orbital magnetic moments in the superconducting condensation, as is seen in the schematic plot in Fig. 1 (b), while in the normal metal case the current populates net magnetic moments at the Fermi energy.

To calculate the current-induced magnetization in both the normal and the superconducting states, we apply the linear response theory and obtain the current-induced bulk magnetization as [38]

$$M_i = - \frac{e}{\hbar} \sum_{\nu} \int_{\text{BZ}} M_{\nu,\mathbf{k},i} v_{\nu,\mathbf{k},j} \left\{ \frac{\tau}{1 - i\omega\tau} \frac{df(\epsilon_{\nu,\mathbf{k}})}{d\epsilon_{\nu,\mathbf{k}}} E_j + \left[ \frac{df(\epsilon_{\nu,\mathbf{k}})}{d\epsilon_{\nu,\mathbf{k}}} - \frac{df(\xi_{\nu,\mathbf{k}})}{d\xi_{\nu,\mathbf{k}}} \right] A_j \right\} \frac{d\mathbf{k}}{(2\pi)^d}. \quad (3)$$

This magnetization is associated with the current density

$$J_i = -\frac{e^2}{\hbar^2} \sum_{\nu} \int_{\text{BZ}} v_{\nu,\mathbf{k},i} v_{\nu,\mathbf{k},j} \left\{ \frac{\tau}{1-i\omega\tau} \frac{df(\epsilon_{\nu,\mathbf{k}})}{d\epsilon_{\nu,\mathbf{k}}} E_j + \left[ \frac{df(\epsilon_{\nu,\mathbf{k}})}{d\epsilon_{\nu,\mathbf{k}}} - \frac{df(\xi_{\nu,\mathbf{k}})}{d\xi_{\nu,\mathbf{k}}} \right] A_j \right\} \frac{d\mathbf{k}}{(2\pi)^d}. \quad (4)$$

Here,  $v_{\nu,\mathbf{k}} = \partial_{\mathbf{k}} \xi_{\nu,\mathbf{k}}$  is the group velocity,  $\tau$  is the effective scattering time,  $d$  is the dimension, and  $f(\epsilon) = \frac{1}{2} (1 - \tanh \frac{1}{2} \beta \epsilon)$  is the Fermi Dirac distribution function with  $k_b$  in  $\beta^{-1} = k_b T$ , the Boltzman constant. The bulk magnetization derived in Eq. 3 involves both the spin and orbital magnetization, and it is applicable in both the normal metal and the superconductivity region. In the normal metal region with zero pairing gap  $\Delta_{\nu,\mathbf{k}} = 0$ , Eq. 4 is the standard Drude formula to describe the current density under an applied electric field  $\mathbf{E}$ , and the current-induced magnetization in Eq. 3 recovers the magnetoelectric susceptibility of a metal [2, 21]. In the superconductivity region with finite pairing gap  $\Delta_{\nu,\mathbf{k}}$ , the first term in both Eq. 3 and 4 approaches zero as the quasiparticle excitations are suppressed by the pairing gap, while the second term that describes the response from condensed Cooper pairs becomes dominant. The supercurrent in Eq. 4 arises from the vector gauge field

$\mathbf{A}$ , in which the pairing phase gradient has been involved through the gauge transformation  $\mathbf{A} \rightarrow \mathbf{A} - \frac{\hbar}{2e} \partial_r \theta$ . Since the vector gauge potential  $\mathbf{A}$  twists the phase  $\theta$  of the pairing condensation, it causes Cooper pairs of net momentum to move [39] so that the pairing condensation carries net magnetization.

For the current-induced magnetization described in Eq. 3 and 4, the vector fields  $\mathbf{E}$  and  $\mathbf{A}$  can further be replaced by the current density  $\mathbf{J}$ , which results in the following expression:

$$M_i = \alpha_{ik} J_k \quad \text{with} \quad \alpha_{ik} = \gamma_{ij} (\tilde{v}^{-1})_{jk}. \quad (5)$$

Here the susceptibility tensor  $\alpha_{ij}$  can be finite only for crystals with point group symmetry belonging to one of the 18 gyrotropic point groups [16, 17], and the tensor  $\gamma_{ij}$ ,  $\tilde{v}_{jk}$  that are used to calculate  $\alpha_{ij}$  can be obtained as

$$\gamma_{ij} = -\frac{e}{\hbar} \sum_{\nu} \int_{\text{BZ}} M_{\nu,\mathbf{k},i} v_{\nu,\mathbf{k},j} \left[ \frac{1}{1-i\omega\tau} \frac{df(\epsilon_{\nu,\mathbf{k}})}{d\epsilon_{\nu,\mathbf{k}}} - \frac{df(\xi_{\nu,\mathbf{k}})}{d\xi_{\nu,\mathbf{k}}} \right] \frac{d\mathbf{k}}{(2\pi)^d}, \quad (6)$$

$$\tilde{v}_{jk} = -\frac{e^2}{\hbar^2} \sum_{\nu} \int_{\text{BZ}} v_{\nu,\mathbf{k},i} v_{\nu,\mathbf{k},j} \left[ \frac{1}{1-i\omega\tau} \frac{df(\epsilon_{\nu,\mathbf{k}})}{d\epsilon_{\nu,\mathbf{k}}} - \frac{df(\xi_{\nu,\mathbf{k}})}{d\xi_{\nu,\mathbf{k}}} \right] \frac{d\mathbf{k}}{(2\pi)^d}. \quad (7)$$

Importantly, both at the zero temperature  $T = 0$  and at finite temperature  $T > T_c$ , it is found that  $\gamma_{ij} \sim \frac{e}{\hbar} \sum_{\nu} \oint M_{\nu,\mathbf{k}_F,i} v_{\nu,\mathbf{k}_F,j} d\mathbf{k}_F$  and  $\tilde{v}_{ij} \sim \frac{e^2}{\hbar^2} \sum_{\nu} \oint v_{\nu,\mathbf{k}_F,i} v_{\nu,\mathbf{k}_F,j} d\mathbf{k}_F$ , with  $\mathbf{k}_F$  the wave vector on the Fermi surfaces, so the induced magnetization  $\mathbf{M}$  at a given current density  $\mathbf{J}$  at  $T = 0$  is the same regardless of whether the system is superconducting or not. At finite temperature  $T > T_c$ , the current-induced magnetization in the normal state can deviate from that in the superconducting state due to the difference in thermal excitations of the two states. Importantly, the group velocity and total magnetic moments of Bloch electrons on the Fermi surfaces are the main decisive factors for the magnetoelectric effect in both the  $T = 0$  superconductivity state and  $T > T_c$  normal metal region. As a result, for a noncentrosymmetric metal that has current-induced orbital magnetization, the orbital magnetization is always maintained in its superconductivity region as long as supercurrent is applied.

Near the superconductivity-normal metal phase transition, the Taylor expansion of pairing gap  $\Delta_{\nu,\mathbf{k}}$  yields  $\gamma_{ij} \sim \frac{e}{\hbar} \sum_{\nu} \oint M_{\nu,\mathbf{k}_F,i} v_{\nu,\mathbf{k}_F,j} |\Delta_{\nu,\mathbf{k}_F}|^2 d\mathbf{k}_F$  and  $\tilde{v}_{ij} \sim \frac{e^2}{\hbar^2} \sum_{\nu} \oint v_{\nu,\mathbf{k}_F,i} v_{\nu,\mathbf{k}_F,j} |\Delta_{\nu,\mathbf{k}_F}|^2 d\mathbf{k}_F$ . Since the small pairing gap there allows quasiparticle excitations to coexist with Cooper pairs, the dependence of pairing gap  $\Delta_{\nu,\mathbf{k}_F}$  on the crystal momentum  $\mathbf{k}$  and band index  $\nu$ , which controls the quasiparticle excitations, can affect the current-induced bulk magnetization. For uniform pairing gap  $\Delta_{\nu,\mathbf{k}} = \Delta_0$ , the current-induced magnetization is exactly the same across the superconductivity normal metal phase transition, while an abrupt change in magnitude can happen in nonuniform pairing cases.

*The orbital magnetoelectric effect in superconducting twisted bilayer graphene.*— In previous studies, supercurrent induced magnetization is purely caused by SOC [1, 1–6, 16]. Recently, superconductivity was observed in TBG which has negligibly small SOC. In this work, we predict a large orbital magnetization can be in-

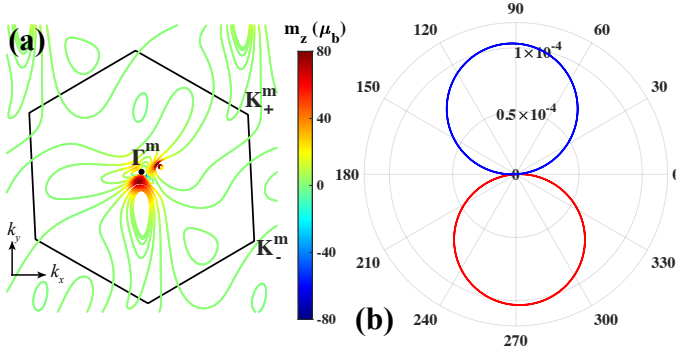


FIG. 2: (a) The orbital magnetic moments at different energy contours of the valence band. The tilted hexagon is the mini-Brillouin zone. Here orbital magnetic moment distribution in one valley is shown, and it can be mapped to the case in the other valley through the time reversal symmetry. (b) The out-of-plane orbital magnetization  $M_z$  (in units of  $\mu_B/\text{nm}^2$ ) induced by in-plane current of  $1\text{ nA/nm}$  along different directions. The red and blue lines mean positive and negative values of orbital magnetization  $M_z$  respectively. The  $x$  direction has been defined to be along the angular bisector between the two zig-zag directions of the top and bottom graphene layers.

duced by a supercurrent in TBG due to the Berry curvatures of the material. This makes TBG an ideal platform to study superconducting orbital magnetoelectric effect introduced in this work.

The TBG aligned with the hBN substrate has the bottom graphene layer couple with the hBN, which breaks the sublattice symmetry, gaps out the Dirac points, and generates finite Berry curvature. With nonzero Berry curvature, the Bloch electrons in the Moiré flat bands become self-rotating and carry orbital magnetic moment as large as tens of Bohr magneton [36]. Due to the mismatch between the hBN and the bottom graphene layer, the equilateral triangle Moiré superlattice has been observed to get deformed [40–42], so the  $C_3$  symmetry of the TBG is generally broken by the strain from the hBN substrate (and we model the strain effect by a uniaxial strain in this work [36]). The resulting TBG system has the lowest  $C_1$  symmetry with finite Berry curvature, which allows the in-plane current to generate an out-of-plane orbital magnetization  $M_z = \alpha_{zx}J_x + \alpha_{zy}J_y$  [36].

To demonstrate the in-plane supercurrent-induced out-of-plane orbital magnetization in a superconducting TBG on hBN, we consider a TBG sample with a twist angle of  $1.6^\circ$ , where uniaxial strain is added along the zig-zag direction in the bottom graphene layer to have it stretched by  $0.1\%$  [38]. With the massive Dirac gap of  $34\text{ meV}$  [43, 44], the Bloch electrons in the valence Moiré flat band carry orbital magnetic moments up to  $80 \mu_B$ , as is shown in Fig. 2 (a). Due to the uniaxial strain from hBN, the distribution of orbital magnetic moments in the mini-Brillouin zone have no  $C_3$  symmetry. With the orbital magnetic moments and group velocity of Bloch

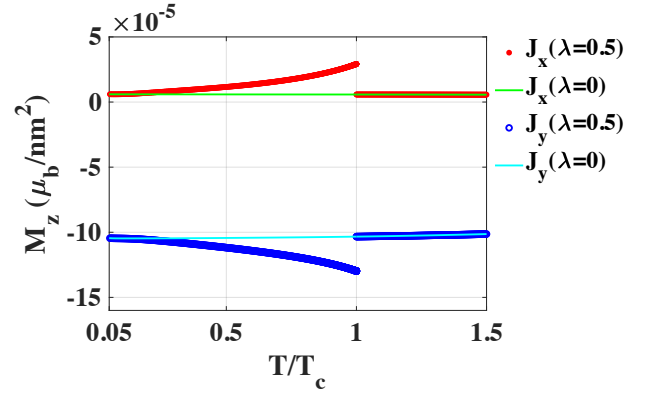


FIG. 3: The current induced out of plane orbital magnetization across the superconductivity normal metal phase transition. The applied current density is taken to be  $1\text{ nA/nm}$ , with direction along  $x$  and  $y$  considered respectively. An abrupt change of  $M_z$  emerges in the case of nonuniform pairing gaps while it keeps the same value across the whole temperature region when the pairing gaps are uniform.

electrons at the Fermi energy, the out-of-plane orbital magnetization at a given in-plane current density is directly computed through Eq. 5-7. Assuming the in-plane supercurrent density to be  $1\text{ nA/nm}$  in the quasi-2D superconducting TBG, we tune the valence Moiré flat band to around  $1/2$  filling and get the generated out of plane orbital magnetization as a function of the in-plane supercurrent direction, which can be seen in Fig. 2 (b). Since the strain has made the large orbital magnetic moments concentrate in the area right below  $\Gamma^m$ , the in-plane supercurrent approximately along the  $y$  direction yields the largest orbital magnetization in the order of  $10^{-4}\mu_B/\text{nm}^2$ . This magnitude of orbital magnetization is comparable to the current induced spin polarization in large Rashba SOC materials, such as Au (111) surfaces and Bi/Ag bilayers [45, 46], so the arising orbital magnetization can be observed experimentally through the optical Kerr effect [47].

Deep in the superconductivity region, at a given current the induced orbital magnetization is approximately the same as that in the normal metallic state regardless of the specific forms of pairing gaps. However, the behavior of current-generated orbital magnetization near the superconducting-normal metal phase transition can be used to further diagnose whether or not the pairing gaps on the Fermi surfaces are uniform. For the superconducting TBG on hBN, we consider the pairing gap on the Fermi surfaces as  $|\Delta_{\nu,\mathbf{k}}| = \Delta_0[1 + \lambda\{\cos(\mathbf{k} \cdot \tilde{\mathbf{a}}_1) + \cos(\mathbf{k} \cdot \tilde{\mathbf{a}}_2) + \cos[\mathbf{k} \cdot (\tilde{\mathbf{a}}_1 - \tilde{\mathbf{a}}_2)]\}]$ , which has been proposed as one of the possible unconventional pairing states for the TBG [48, 49]. Here  $\Delta_0 = 1.76k_B T_c \tanh\left(1.78\sqrt{\frac{T_c}{T}} - 1\right)$  and  $\tilde{\mathbf{a}}_1, \tilde{\mathbf{a}}_2$  are the primitive lattice vectors for the deformed Moiré

superlattice, as defined in the Supplementary Materials [38]. At  $\lambda = 0$ , the pairing gap is uniform, so the current-generated out-of-plane orbital magnetization smoothly connects to that in the normal metal region, while the nonuniform pairing gap at  $\lambda = 0.5$  develops an abrupt jump in magnitude of  $M_z$  at  $T_c$ , as is shown in Fig. 3. This is consistent with our analysis and can be used to diagnose the uniformity of pairing gaps in TBG on hBN.

*Discussion.*— It is important to note that our theory applies to a large number of recently discovered superconductors with Berry curvatures and negligible SOC, such as a trilayer graphene Moiré superlattice on hBN [50–53], bilayer graphene/hBN superlattices [54], and twisted double bilayer graphene [55, 56]. Moreover, our theory also applies to non-centrosymmetric superconductors with strong SOC and finite Berry curvatures such as chiral crystals,  $\text{Li}_2\text{Pt}_3\text{B}$  [57],  $\text{Li}_2\text{Pd}_3\text{B}$  [58],  $\text{Mo}_3\text{Al}_2\text{C}$  [59],  $\text{TaRh}_2\text{B}_2$  and  $\text{NbRh}_2\text{B}_2$  [60], which were recently discovered to have superconductivity. In these chiral crystals the orbital magnetic moment carried by the Bloch electrons originates from the Weyl SOC [61], so the spin and orbital magnetization are strongly mixed and the orbital magnetization effect cannot be ignored.

*Acknowledgement.*— The authors would like to thank K. F. Mak for inspiring discussions. K. T. Law acknowledges the support of the Croucher Foundation and HKRGC through C6025-19G, 16310219 and 16309718.

---

\* wenyuhe@mit.edu

† phlaw@ust.hk

- [1] L. S. Levitov, Yu. V. Nazarov, and G. M. Eliashberg, Pis'ma Zh. Eksp. Teor. Fiz. **41** 365 (1985).
- [2] V. M. Edel'shtein, Zh. Eksp. Teor. Fiz. **95**, 2151 (1989).
- [3] V. M. Edelstein, Phys. Rev. Lett. **75**, 2004 (1995).
- [4] S. K. Yip, Phys. Rev. B **65**, 144508 (2002).
- [5] K. V. Samokhin, Phys. Rev. B **70**, 104521 (2004).
- [6] S. Fujimoto, Phys. Rev. B **72**, 024515 (2005).
- [7] E. Bauer and M. Sigrist, Noncentrosymmetric Superconductors (Springer, Berlin, 2012).
- [8] G. Takachov, Phys. Rev. Lett. **118**, 016802 (2017).
- [9] D. Xiao, M.-C. Chang, and Q. Niu, Rev. Mod. Phys. **82**, 1959 (2010).
- [10] M.-C. Chang, and Q. Niu, Phys. Rev. B **53**, 7010 (1996).
- [11] G. Sundaram, and Q. Niu, Phys. Rev. B **59**, 14915 (1999).
- [12] D. Xiao, J. Shi, and Q. Niu, Phys. Rev. Lett. **95**, 137204 (2005).
- [13] J. Shi, G. Vignale, D. Xiao, and Q. Niu, Phys. Rev. Lett. **99**, 197202 (2007).
- [14] T. Thonhauser, D. Ceresoli, D. Vanderbilt, and R. Resta, Phys. Rev. Lett. **95**, 137205 (2005).
- [15] D. Ceresoli, T. Thonhauser, D. Vanderbilt, and R. Resta, Phys. Rev. B **74**, 024408 (2006).
- [16] W.-Y. He, and K. T. Law, Phys. Rev. Research **2**, 012073 (R) (2020).
- [17] F. de Juan, A. G. Grushin, T. Morimoto, and J. E. Moore, Nat. Commun. **8**, 15995 (2017).
- [18] L. S. Levitov, Yu. V. Nazarov, and G. M. Eliashberg, Zh. Eksp. Teor. Fiz. **88**, 229 (1985).
- [19] V. M. Edelstein, Solid State Commun. **73**, 233 (1990).
- [20] S. Zhong, J. E. Moore, I. Souza, Phys. Rev. Lett. **116**, 235205 (2015).
- [21] J. Ma, and D. A. Pesin, Phys. Rev. B **92**, 235205 (2015).
- [22] Y. Cao et al., Nature (London) **566**, 43 (2018).
- [23] M. Yankowitz et al., Science **363**, 1059 (2019).
- [24] E. Codecido et al., Sci. Adv. **5**, eaaw9770 (2019).
- [25] X. Lu et al., Nature **574**, 653 (2019).
- [26] Y. Saito, J. Ge, K. Watanabe, T. Taniguchi, and A. F. Young, Nat. Phys. **16**, 926 (2020).
- [27] P. Stepanov et al., Nature **583**, 375 (2020).
- [28] A. L. Sharpe et al., Science **365**, 605 (2019).
- [29] M. Serlin et al., Science **367**, 900 (2019).
- [30] H. Polshyn et al., arXiv: 2004.11353.
- [31] C. L. Tschirhart et al., arXiv: 2006.08053.
- [32] M. Xie, and A. H. MacDonald, Phys. Rev. Lett. **124**, 097601 (2020).
- [33] Y.-H. Zhang, D. Mao, T. Senthil, Phys. Rev. Research **1**, 033126 (2019).
- [34] Y.-H. Zhang, D. Mao, Y. Cao, P.-J. Herrero, and T. Senthil, Phys. Rev. B **99**, 075127 (2019).
- [35] N. Bultinck, S. Chatterjee, and M. P. Zaletel, Phys. Rev. Lett. **124**, 166601 (2020).
- [36] W.-Y. He, D. G.-Gordon, and K. T. Law, Nat. Commun. **11**, 1650 (2020).
- [37] A. Ramires, and M. Sigrist, Phys. Rev. B **94**, 104501 (2016).
- [38] See the Supplemental Material for (i) the details about the Bogliubov-de Gennes Hamiltonian in Eigen band basis, (ii) the detailed derivation of the current induced magnetization in both the normal metal and superconductivity region, (iii) the continuum model of twisted bilayer graphene on boron nitride with uniaxial strain.
- [39] The pairing phase gradient in superconductivity order parameter is directly related to the net momentum of a Cooper pair, which can be easily seen by the Fourier transformation  $\sum_q q \Delta_{\nu,k,q}^* \Delta_{\nu,k,q} = \frac{1}{2} [(\partial_r \Delta_{\nu,k,r}^*) \Delta_{\nu,k,r} - \Delta_{\nu,k,r}^* (\partial_r \Delta_{\nu,k,r})] = |\Delta_{\nu,k}|^2 \partial_r \theta$ . Here the pairing order amplitude is uniform in the space  $\Delta_{\nu,k,r} = \Delta_{\nu,k} e^{-i\theta}$  but the phase  $\theta$  depends on  $r$ .
- [40] Y. Choi et al., Nat. Phys. **15**, 1174 (2019).
- [41] A. Kerelsky et al., Nature **572**, 95 (2019).
- [42] Y. Xie et al., Nature **572**, 101 (2019).
- [43] M. Lee et al., Science **353**, 1526 (2016).
- [44] H. Kim et al., Nano Lett. **18**, 7732 (2018).
- [45] A. Johansson, J. Henk, and I. Mertig, Phys. Rev. B **93**, 195440 (2016).
- [46] A. Johansson, J. Henk, and I. Mertig, Phys. Rev. B **97**, 085417 (2018).
- [47] J. Lee, Z. Wang, H. Xie, K. F. Mak, and J. Shan, Nat. Mater. **16**, 887 (2017).
- [48] B. Lian, Z. Wang, and B. A. Bernevig, Phys. Rev. Lett. **122**, 257002 (2019).
- [49] F. Wu and S. D. Sarma, Phys. Rev. B **99**, 220507 (R) (2019).
- [50] G. Chen et al., Nature **572**, 215 (2019).
- [51] K.-T. Tsai et al., arXiv: 1912.03375.
- [52] Y. Shi et al. arXiv: 2004.12414.
- [53] J. M. Park et al. arXiv: 2012.01434.

- [54] S. Moriyama et al., arXiv: 1901.09356.
- [55] X. Liu et al., *Nature* **583**, 221 (2020).
- [56] C. Shen et al., *Nat. Phys.* **16**, 520 (2020).
- [57] H. Q. Yuan et al., *Phys. Rev. Lett.* **97**, 017006 (2006).
- [58] K. Togano et al., *Phys. Rev. Lett.* **93**, 247004 (2004).
- [59] A. B. Karki et al., *Phys. Rev. B* **82**, 064512 (2010).
- [60] E. M. Carnicom et al., *Sci. Adv.* **4**, 7969 (2018).
- [61] G. Chang et al., *Nat. Mater.* **17**, 978 (2018).

# Supplementary Material for “Superconducting Orbital Magnetoelectric Effect and the Case Study of Twisted Bilayer Graphene”

## BOGLIUBOV-DE GENNES HAMILTONIAN AND THE GREEN’S FUNCTION

The generic Hamiltonian that can describe the normal state of a system takes the form

$$\mathcal{H}_0 = \sum_{\nu, \nu', \mathbf{k}} c_{\nu, \mathbf{k}}^\dagger H_{0, \nu \nu'} c_{\nu', \mathbf{k}}, \quad (\text{S1})$$

with  $c_{\nu, \mathbf{k}}^\dagger$  ( $c_{\nu, \mathbf{k}}$ ) being the creation (annihilation) operator,  $H_{0, \nu \nu'}(\mathbf{k})$  being the element of the Hamiltonian matrix  $H_0(\mathbf{k})$ , and  $\nu = 1, 2, 3, \dots$  denoting the spin, orbital index of the system. The Bogliubov-de Gennes Hamiltonian that can describe the superconductivity state of the system is

$$\mathcal{H} = \frac{1}{2} \sum_{\mathbf{k}} \begin{pmatrix} c_{\mathbf{k}}^\dagger & c_{-\mathbf{k}} \end{pmatrix} \begin{pmatrix} H_0(\mathbf{k}) & \hat{\Delta}(\mathbf{k}) \\ \hat{\Delta}^\dagger(\mathbf{k}) & -H_0^*(-\mathbf{k}) \end{pmatrix} \begin{pmatrix} c_{\mathbf{k}} \\ c_{-\mathbf{k}}^\dagger \end{pmatrix}, \quad (\text{S2})$$

where  $c_{\mathbf{k}} = [c_{1, \mathbf{k}}, c_{2, \mathbf{k}}, c_{3, \mathbf{k}}, \dots]^\text{T}$ ,  $c_{\mathbf{k}}^\dagger = [c_{1, \mathbf{k}}^\dagger, c_{2, \mathbf{k}}^\dagger, c_{3, \mathbf{k}}^\dagger, \dots]$ , and  $\hat{\Delta}(\mathbf{k})$  is the pairing matrix. We know that the normal state Hamiltonian  $H_0(\mathbf{k})$  can be diagonalized by a unitary transformation  $U(\mathbf{k})$  as

$$U(\mathbf{k}) H_0(\mathbf{k}) U^\dagger(\mathbf{k}) = \text{diag}[\xi_{1, \mathbf{k}}, \xi_{2, \mathbf{k}}, \dots, \xi_{\nu, \mathbf{k}}], \quad (\text{S3})$$

with  $U^\dagger(\mathbf{k}) U(\mathbf{k}) = 1$  and the corresponding eigen states  $\phi_{\nu, \mathbf{k}} = U_{\nu \nu'}(\mathbf{k}) c_{\nu', \mathbf{k}}$ ,  $\phi_{\nu, \mathbf{k}}^\dagger = c_{\nu', \mathbf{k}}^\dagger U_{\nu' \nu}^*(\mathbf{k})$ . Applying the unitary transformation to the Bogliubov-de Gennes Hamiltonian then yields

$$\begin{pmatrix} U_{\mathbf{k}} & 0 \\ 0 & U_{-\mathbf{k}}^* \end{pmatrix} \begin{pmatrix} H_0(\mathbf{k}) & \hat{\Delta}_{\mathbf{k}} \\ \hat{\Delta}_{\mathbf{k}}^\dagger & -H_0^*(-\mathbf{k}) \end{pmatrix} \begin{pmatrix} U_{\mathbf{k}}^\dagger & 0 \\ 0 & U_{-\mathbf{k}}^\text{T} \end{pmatrix} = \begin{pmatrix} U_{\mathbf{k}} H_0(\mathbf{k}) U_{\mathbf{k}}^\dagger & U_{\mathbf{k}} \hat{\Delta}_{\mathbf{k}} U_{-\mathbf{k}}^\text{T} \\ U_{-\mathbf{k}}^* \hat{\Delta}_{\mathbf{k}}^\dagger U_{\mathbf{k}}^\dagger & -U_{-\mathbf{k}}^* H_0^*(-\mathbf{k}) U_{-\mathbf{k}}^\text{T} \end{pmatrix}. \quad (\text{S4})$$

Importantly, after the unitary transformation, we obtain

$$U_{\mathbf{k}} H_0(\mathbf{k}) U_{\mathbf{k}}^\dagger = \text{diag}[\xi_{1, \mathbf{k}}, \xi_{2, \mathbf{k}}, \dots, \xi_{\nu, \mathbf{k}}], \quad -U_{-\mathbf{k}}^* H_0^*(-\mathbf{k}) U_{-\mathbf{k}}^\text{T} = \text{diag}[-\xi_{1, -\mathbf{k}}, -\xi_{2, -\mathbf{k}}, \dots, -\xi_{\nu, -\mathbf{k}}]. \quad (\text{S5})$$

In such eigen-band basis  $[\phi_{1, \mathbf{k}}^\dagger, \phi_{2, \mathbf{k}}^\dagger, \dots, \phi_{\nu, \mathbf{k}}^\dagger, \phi_{1, -\mathbf{k}}, \phi_{2, -\mathbf{k}}, \dots, \phi_{\nu, -\mathbf{k}}]$ , the intraband pairing  $\langle \phi_{\nu, -\mathbf{k}} \phi_{\nu, \mathbf{k}} \rangle$  gives the energetically favourable pairing phase while other interband pairing will require extra attractive interaction to overcome the energy (momentum) difference [S1]. In the energetically favourable pairing phase, the pairing matrix respects  $H_0(\mathbf{k}) \hat{\Delta}_{\mathbf{k}} - \hat{\Delta}_{\mathbf{k}} H_0^*(-\mathbf{k}) = 0$  [S1] and the pairing matrix is therefore diagonalized simultaneously by the unitary transformation as

$$U_{\mathbf{k}} \hat{\Delta}_{\mathbf{k}} U_{-\mathbf{k}}^\text{T} = \text{diag}[\Delta_{1, \mathbf{k}}, \Delta_{2, \mathbf{k}}, \dots, \Delta_{\nu, \mathbf{k}}], \quad U_{-\mathbf{k}}^* \hat{\Delta}_{\mathbf{k}}^\dagger U_{\mathbf{k}}^\dagger = \text{diag}[\Delta_{1, \mathbf{k}}^*, \Delta_{2, \mathbf{k}}^*, \dots, \Delta_{\nu, \mathbf{k}}^*]. \quad (\text{S6})$$

As a result, the Bogliubov-de Gennes Hamiltonian in the eigen-band basis takes the form

$$\begin{pmatrix} U_{\mathbf{k}} & 0 \\ 0 & U_{-\mathbf{k}}^* \end{pmatrix} \begin{pmatrix} H_0(\mathbf{k}) & \hat{\Delta}_{\mathbf{k}} \\ \hat{\Delta}_{\mathbf{k}}^\dagger & -H_0^*(-\mathbf{k}) \end{pmatrix} \begin{pmatrix} U_{\mathbf{k}}^\dagger & 0 \\ 0 & U_{-\mathbf{k}}^\text{T} \end{pmatrix} = \begin{pmatrix} \xi_{1, \mathbf{k}} & 0 & 0 & 0 & \Delta_{1, \mathbf{k}} & 0 & 0 & 0 \\ 0 & \xi_{2, \mathbf{k}} & 0 & 0 & 0 & \Delta_{2, \mathbf{k}} & 0 & 0 \\ 0 & 0 & \dots & 0 & 0 & 0 & \dots & 0 \\ 0 & 0 & 0 & \xi_{\nu, \mathbf{k}} & 0 & 0 & 0 & \Delta_{\nu, \mathbf{k}} \\ \Delta_{1, \mathbf{k}}^* & 0 & 0 & 0 & -\xi_{1, -\mathbf{k}} & 0 & 0 & 0 \\ 0 & \Delta_{2, \mathbf{k}}^* & 0 & 0 & 0 & -\xi_{2, -\mathbf{k}} & 0 & 0 \\ 0 & 0 & \dots & 0 & 0 & 0 & \dots & 0 \\ 0 & 0 & 0 & \Delta_{\nu, \mathbf{k}}^* & 0 & 0 & 0 & -\xi_{\nu, -\mathbf{k}} \end{pmatrix}. \quad (\text{S7})$$

We define the Green’s function for the Bogliubov-de Gennes Hamiltonian as

$$G_0^{-1}(\mathbf{k}, i\omega_n) = \begin{pmatrix} i\omega_n - H_0(\mathbf{k}) & -\hat{\Delta}_{\mathbf{k}} \\ -\hat{\Delta}_{\mathbf{k}} & i\omega_n + H_0^*(-\mathbf{k}) \end{pmatrix}, \quad \text{and} \quad G_0(\mathbf{k}, i\omega_n) = \begin{pmatrix} G_e(\mathbf{k}, i\omega_n) & F(\mathbf{k}, i\omega_n) \\ F^\dagger(\mathbf{k}, i\omega_n) & G_h(\mathbf{k}, i\omega_n) \end{pmatrix}, \quad (\text{S8})$$

and then apply the unitary transformation to the Green's function

$$\begin{pmatrix} U_{\mathbf{k}} & 0 \\ 0 & U_{-\mathbf{k}}^* \end{pmatrix} \begin{pmatrix} G_e(\mathbf{k}, i\omega_n) & F(\mathbf{k}, i\omega_n) \\ F^\dagger(\mathbf{k}, i\omega_n) & G_h(\mathbf{k}, i\omega_n) \end{pmatrix} \begin{pmatrix} U_{\mathbf{k}}^\dagger & 0 \\ 0 & U_{-\mathbf{k}}^T \end{pmatrix} = \begin{pmatrix} U_{\mathbf{k}} G_e(\mathbf{k}, i\omega_n) U_{\mathbf{k}}^\dagger & U_{\mathbf{k}} F(\mathbf{k}, i\omega_n) U_{-\mathbf{k}}^T \\ U_{-\mathbf{k}}^* F^\dagger(\mathbf{k}, i\omega_n) U_{\mathbf{k}}^\dagger & U_{-\mathbf{k}}^* G_h(\mathbf{k}, i\omega_n) U_{-\mathbf{k}}^T \end{pmatrix}. \quad (\text{S9})$$

which gives

$$U_{\mathbf{k}} G_e(\mathbf{k}, i\omega_n) U_{\mathbf{k}}^\dagger = \begin{pmatrix} -\frac{i\omega_n + \xi_{1,\mathbf{k}}}{\omega_n^2 + \xi_{1,\mathbf{k}}^2 + \Delta_{1,\mathbf{k}} \Delta_{1,\mathbf{k}}^*} & 0 & 0 & 0 \\ 0 & -\frac{i\omega_n + \xi_{2,\mathbf{k}}}{\omega_n^2 + \xi_{2,\mathbf{k}}^2 + \Delta_{2,\mathbf{k}} \Delta_{2,\mathbf{k}}^*} & 0 & 0 \\ 0 & 0 & \dots & 0 \\ 0 & 0 & 0 & -\frac{i\omega_n + \xi_{\nu,\mathbf{k}}}{\omega_n^2 + \xi_{\nu,\mathbf{k}}^2 + \Delta_{\nu,\mathbf{k}} \Delta_{\nu,\mathbf{k}}^*} \end{pmatrix}, \quad (\text{S10})$$

$$U_{\mathbf{k}} F(\mathbf{k}, i\omega_n) U_{-\mathbf{k}}^T = \begin{pmatrix} -\frac{\Delta_{1,\mathbf{k}}}{\omega_n^2 + \xi_{1,\mathbf{k}}^2 + \Delta_{1,\mathbf{k}} \Delta_{1,\mathbf{k}}^*} & 0 & 0 & 0 \\ 0 & -\frac{\Delta_{2,\mathbf{k}}}{\omega_n^2 + \xi_{2,\mathbf{k}}^2 + \Delta_{2,\mathbf{k}} \Delta_{2,\mathbf{k}}^*} & 0 & 0 \\ 0 & 0 & \dots & 0 \\ 0 & 0 & 0 & -\frac{\Delta_{\nu,\mathbf{k}}}{\omega_n^2 + \xi_{\nu,\mathbf{k}}^2 + \Delta_{\nu,\mathbf{k}} \Delta_{\nu,\mathbf{k}}^*} \end{pmatrix}, \quad (\text{S11})$$

$$U_{-\mathbf{k}}^* F^\dagger(\mathbf{k}, i\omega_n) U_{\mathbf{k}}^\dagger = \begin{pmatrix} -\frac{\Delta_{1,\mathbf{k}}^*}{\omega_n^2 + \xi_{1,\mathbf{k}}^2 + \Delta_{1,\mathbf{k}} \Delta_{1,\mathbf{k}}^*} & 0 & 0 & 0 \\ 0 & -\frac{\Delta_{2,\mathbf{k}}^*}{\omega_n^2 + \xi_{2,\mathbf{k}}^2 + \Delta_{2,\mathbf{k}} \Delta_{2,\mathbf{k}}^*} & 0 & 0 \\ 0 & 0 & \dots & 0 \\ 0 & 0 & 0 & -\frac{\Delta_{\nu,\mathbf{k}}^*}{\omega_n^2 + \xi_{\nu,\mathbf{k}}^2 + \Delta_{\nu,\mathbf{k}} \Delta_{\nu,\mathbf{k}}^*} \end{pmatrix}, \quad (\text{S12})$$

$$U_{-\mathbf{k}}^* G_h(\mathbf{k}, i\omega_n) U_{-\mathbf{k}}^T = \begin{pmatrix} -\frac{i\omega_n - \xi_{1,\mathbf{k}}}{\omega_n^2 + \xi_{1,\mathbf{k}}^2 + \Delta_{1,\mathbf{k}} \Delta_{1,\mathbf{k}}^*} & 0 & 0 & 0 \\ 0 & -\frac{i\omega_n - \xi_{2,\mathbf{k}}}{\omega_n^2 + \xi_{2,\mathbf{k}}^2 + \Delta_{2,\mathbf{k}} \Delta_{2,\mathbf{k}}^*} & 0 & 0 \\ 0 & 0 & \dots & 0 \\ 0 & 0 & 0 & -\frac{i\omega_n - \xi_{\nu,\mathbf{k}}}{\omega_n^2 + \xi_{\nu,\mathbf{k}}^2 + \Delta_{\nu,\mathbf{k}} \Delta_{\nu,\mathbf{k}}^*} \end{pmatrix}. \quad (\text{S13})$$

## LINEAR RESPONSE THEORY FOR THE CURRENT INDUCED MAGNETIZATION

Applying current introduces a perturbation

$$\delta\mathcal{H} = - \sum_{\mathbf{k}, \mathbf{q}} c_{\mathbf{k}-\frac{1}{2}\mathbf{q}}^\dagger c_{\mathbf{k}+\frac{1}{2}\mathbf{q}} \left[ \frac{e}{\hbar} \partial_{k_i} H_0(\mathbf{k}) A_i(-\mathbf{q}, t) - \frac{e^2}{2\hbar^2} \partial_{k_i k_j}^2 H_0(\mathbf{k}) A_i(\mathbf{q}, t) A_j(-\mathbf{q}, t) \right] \quad (\text{S14})$$

to the Bogliubov-de Gennes Hamiltonian, so the free energy density of the system get changed. The change of free energy density can be obtained through expanding the electromagnetic gauge fields and it reads

$$\begin{aligned} \Delta F &= \frac{1}{2} \sum_{\mathbf{q}, m} A_i(-\mathbf{q}, -i\omega_m) \Pi_{ij}(\mathbf{q}, i\omega_m) A_j(\mathbf{q}, i\omega_m) \\ &+ \frac{1}{2} \sum_{\mathbf{q}, m} B_i(-\mathbf{q}, -i\omega_m) T_{ij}^s(\mathbf{q}, i\omega_m) A_j(\mathbf{q}, i\omega_m) + \frac{1}{2} \sum_{\mathbf{q}, m} A_i(-\mathbf{q}, -i\omega_m) \tilde{T}_{ij}^s(\mathbf{q}, i\omega_m) B_j(\mathbf{q}, i\omega_m). \end{aligned} \quad (\text{S15})$$

Here the terms  $T_{ij}^s(\mathbf{q}, i\omega_m)$  and  $\tilde{T}_{ij}^s(\mathbf{q}, i\omega_m)$

$$\begin{aligned} T_{ij}^s(\mathbf{q}, i\omega_m) &= \frac{1}{\beta V} \sum_{\mathbf{k}, n} \text{tr} \left[ G_e \left( \mathbf{k} - \frac{1}{2}\mathbf{q}, i\omega_n \right) \frac{1}{2} \mu_b g \sigma_i G_e \left( \mathbf{k} + \frac{1}{2}\mathbf{q}, i\omega_n + i\omega_m \right) \frac{e}{\hbar} \frac{\partial H_0(\mathbf{k})}{\partial k_j} \right. \\ &\quad \left. - F \left( \mathbf{k} - \frac{1}{2}\mathbf{q}, i\omega_n \right) \frac{1}{2} \mu_b g \sigma_i^* F^\dagger \left( \mathbf{k} + \frac{1}{2}\mathbf{q}, i\omega_n + i\omega_m \right) \frac{e}{\hbar} \frac{\partial H_0(\mathbf{k})}{\partial k_j} \right], \end{aligned} \quad (\text{S16})$$

$$\begin{aligned} \tilde{T}_{ij}^s(\mathbf{q}, i\omega_m) &= \frac{1}{\beta V} \sum_{\mathbf{k}, n} \text{tr} \left[ G_e \left( \mathbf{k} - \frac{1}{2}\mathbf{q}, i\omega_n \right) \frac{e}{\hbar} \frac{\partial H_0(\mathbf{k})}{\partial k_i} G_e \left( \mathbf{k} + \frac{1}{2}\mathbf{q}, i\omega_n + i\omega_m \right) \frac{1}{2} \mu_b g \sigma_j \right. \\ &\quad \left. - F \left( \mathbf{k} - \frac{1}{2}\mathbf{q}, i\omega_n \right) \frac{e}{\hbar} \frac{\partial H_0^*(-\mathbf{k})}{\partial k_i} F_0^\dagger \left( \mathbf{k} + \frac{1}{2}\mathbf{q}, i\omega_n + i\omega_m \right) \frac{1}{2} \mu_b g \sigma_j \right]. \end{aligned} \quad (\text{S17})$$



give the spin magnetoelectric susceptibility in both the superconductivity and normal metal region, while the polarization tensor  $\Pi_{ij}(\mathbf{q}, i\omega_m)$

$$\begin{aligned} \Pi_{ij}(\mathbf{q}, i\omega_m) = & \frac{1}{\beta V} \sum_{\mathbf{k}, n} \text{tr} \left[ G_e(\mathbf{k}, i\omega_n) \frac{e^2}{\hbar^2} \frac{\partial^2 H_0(\mathbf{k})}{\partial k_i \partial k_j} + G_e\left(\mathbf{k} - \frac{1}{2}\mathbf{q}, i\omega_n\right) \frac{e}{\hbar} \frac{\partial H_0(\mathbf{k})}{\partial k_i} G_e\left(\mathbf{k} + \frac{1}{2}\mathbf{q}, i\omega_n + i\omega_m\right) \frac{e}{\hbar} \frac{\partial H_0(\mathbf{k})}{\partial k_j} \right. \\ & \left. + F\left(\mathbf{k} - \frac{1}{2}\mathbf{q}, i\omega_n\right) \frac{e}{\hbar} \frac{\partial H_0^*(-\mathbf{k})}{\partial k_i} F^\dagger\left(\mathbf{k} + \frac{1}{2}\mathbf{q}, i\omega_n + i\omega_m\right) \frac{e}{\hbar} \frac{\partial H_0(\mathbf{k})}{\partial k_j} \right], \end{aligned} \quad (\text{S18})$$

is responsible for the current and current induced orbital magnetization in both the superconductivity and normal metal region.

### Polarization Tensor, Current, and the Current Induced Orbital Magnetization

Substituting Eq. S10, S11, S12, S13 into Eq. S18, we can obtain the polarization tensor  $\Pi_{ij}(\mathbf{q}, i\omega_m)$  to be

$$\Pi_{ij}(\mathbf{q}, i\omega_m) = \Pi_{ij}^{\text{sta}}(\mathbf{q}) + \Pi_{ij}^{\text{dyn}}(\mathbf{q}, i\omega_m),$$

with the static part  $\Pi_{ij}^{\text{sta}}(\mathbf{q})$

$$\begin{aligned} \Pi_{ij}^{\text{sta}}(\mathbf{q}) = & \frac{1}{2V} \frac{e^2}{\hbar^2} \sum_{\mathbf{k}, \nu} \left[ \frac{\epsilon_{\nu, \mathbf{k}} + \xi_{\nu, \mathbf{k}}}{\epsilon_{\nu, \mathbf{k}}} f(\epsilon_{\nu, \mathbf{k}}) + \frac{\epsilon_{\nu, \mathbf{k}} - \xi_{\nu, \mathbf{k}}}{\epsilon_{\nu, \mathbf{k}}} f(-\epsilon_{\nu, \mathbf{k}}) \right] \langle \phi_{\nu, \mathbf{k}} | \partial_{k_i}^2 H_0(\mathbf{k}) | \phi_{\nu, \mathbf{k}} \rangle \\ & - \frac{1}{2V} \frac{e^2}{\hbar^2} \sum_{\mathbf{k}, \nu, \nu'} \left[ \left( 1 - \frac{\xi_{\nu, \mathbf{k} - \frac{1}{2}\mathbf{q}} \xi_{\nu', \mathbf{k} + \frac{1}{2}\mathbf{q}} + \Delta_{\nu, \mathbf{k} - \frac{1}{2}\mathbf{q}} \Delta_{\nu', \mathbf{k} + \frac{1}{2}\mathbf{q}}^*}{\epsilon_{\nu', \mathbf{k} + \frac{1}{2}\mathbf{q}} \epsilon_{\nu, \mathbf{k} - \frac{1}{2}\mathbf{q}}} \right) \frac{1 - f(\epsilon_{\nu', \mathbf{k} + \frac{1}{2}\mathbf{q}}) - f(\epsilon_{\nu, \mathbf{k} - \frac{1}{2}\mathbf{q}})}{\epsilon_{\nu', \mathbf{k} + \frac{1}{2}\mathbf{q}} + \epsilon_{\nu, \mathbf{k} - \frac{1}{2}\mathbf{q}}} \right. \\ & \left. - \left( 1 + \frac{\xi_{\nu, \mathbf{k} - \frac{1}{2}\mathbf{q}} \xi_{\nu', \mathbf{k} + \frac{1}{2}\mathbf{q}} + \Delta_{\nu, \mathbf{k} - \frac{1}{2}\mathbf{q}} \Delta_{\nu', \mathbf{k} + \frac{1}{2}\mathbf{q}}^*}{\epsilon_{\nu', \mathbf{k} + \frac{1}{2}\mathbf{q}} \epsilon_{\nu, \mathbf{k} - \frac{1}{2}\mathbf{q}}} \right) \frac{f(\epsilon_{\nu', \mathbf{k} + \frac{1}{2}\mathbf{q}}) - f(\epsilon_{\nu, \mathbf{k} - \frac{1}{2}\mathbf{q}})}{\epsilon_{\nu', \mathbf{k} + \frac{1}{2}\mathbf{q}} - \epsilon_{\nu, \mathbf{k} - \frac{1}{2}\mathbf{q}}} \right] \\ & \langle \phi_{\nu, \mathbf{k} - \frac{1}{2}\mathbf{q}} | \partial_{k_i} H_0(\mathbf{k}) | \phi_{\nu', \mathbf{k} + \frac{1}{2}\mathbf{q}} \rangle \langle \phi_{\nu', \mathbf{k} + \frac{1}{2}\mathbf{q}} | \partial_{k_j} H_0(\mathbf{k}) | \phi_{\nu, \mathbf{k} - \frac{1}{2}\mathbf{q}} \rangle, \end{aligned} \quad (\text{S19})$$

and the dynamical part  $\Pi_{ij}^{\text{dyn}}(\mathbf{q}, i\omega_m)$

$$\begin{aligned} \Pi_{ij}^{\text{dyn}}(\mathbf{q}, i\omega_m) = & \frac{1}{4V} \sum_{\mathbf{k}, \nu, \nu'} \left\{ \left( 1 - \frac{\xi_{\nu, \mathbf{k} - \frac{1}{2}\mathbf{q}} \xi_{\nu', \mathbf{k} + \frac{1}{2}\mathbf{q}} + \Delta_{\nu, \mathbf{k} - \frac{1}{2}\mathbf{q}} \Delta_{\nu', \mathbf{k} + \frac{1}{2}\mathbf{q}}^*}{\epsilon_{\nu', \mathbf{k} + \frac{1}{2}\mathbf{q}} \epsilon_{\nu, \mathbf{k} - \frac{1}{2}\mathbf{q}}} \right) \left[ \frac{i\omega_m}{i\omega_m + \epsilon_{\nu', \mathbf{k} + \frac{1}{2}\mathbf{q}} + \epsilon_{\nu, \mathbf{k} - \frac{1}{2}\mathbf{q}}} + \frac{i\omega_m}{i\omega_m - (\epsilon_{\nu', \mathbf{k} + \frac{1}{2}\mathbf{q}} + \epsilon_{\nu, \mathbf{k} - \frac{1}{2}\mathbf{q}})} \right] \right. \\ & \frac{1 - f(\epsilon_{\nu', \mathbf{k} + \frac{1}{2}\mathbf{q}}) - f(\epsilon_{\nu, \mathbf{k} - \frac{1}{2}\mathbf{q}})}{\epsilon_{\nu', \mathbf{k} + \frac{1}{2}\mathbf{q}} + \epsilon_{\nu, \mathbf{k} - \frac{1}{2}\mathbf{q}}} \\ & - \left( 1 + \frac{\xi_{\nu, \mathbf{k} - \frac{1}{2}\mathbf{q}} \xi_{\nu', \mathbf{k} + \frac{1}{2}\mathbf{q}} + \Delta_{\nu, \mathbf{k} - \frac{1}{2}\mathbf{q}} \Delta_{\nu', \mathbf{k} + \frac{1}{2}\mathbf{q}}^*}{\epsilon_{\nu', \mathbf{k} + \frac{1}{2}\mathbf{q}} \epsilon_{\nu, \mathbf{k} - \frac{1}{2}\mathbf{q}}} \right) \left[ \frac{i\omega_m}{i\omega_m - (\epsilon_{\nu', \mathbf{k} + \frac{1}{2}\mathbf{q}} - \epsilon_{\nu, \mathbf{k} - \frac{1}{2}\mathbf{q}})} + \frac{i\omega_m}{i\omega_m + \epsilon_{\nu', \mathbf{k} + \frac{1}{2}\mathbf{q}} - \epsilon_{\nu, \mathbf{k} - \frac{1}{2}\mathbf{q}}} \right] \\ & \left. \frac{f(\epsilon_{\nu', \mathbf{k} + \frac{1}{2}\mathbf{q}}) - f(\epsilon_{\nu, \mathbf{k} - \frac{1}{2}\mathbf{q}})}{\epsilon_{\nu', \mathbf{k} + \frac{1}{2}\mathbf{q}} - \epsilon_{\nu, \mathbf{k} - \frac{1}{2}\mathbf{q}}} \right\} \langle \phi_{\nu, \mathbf{k} - \frac{1}{2}\mathbf{q}} | \frac{e}{\hbar} \partial_{k_i} H_0(\mathbf{k}) | \phi_{\nu', \mathbf{k} + \frac{1}{2}\mathbf{q}} \rangle \langle \phi_{\nu', \mathbf{k} + \frac{1}{2}\mathbf{q}} | \frac{e}{\hbar} \partial_{k_j} H_0(\mathbf{k}) | \phi_{\nu, \mathbf{k} - \frac{1}{2}\mathbf{q}} \rangle. \end{aligned} \quad (\text{S20})$$

The static and dynamic part of the polarization tensor can be expanded in terms of  $\mathbf{q}$  to the linear order as

$$\Pi_{ij}^{\text{sta}}(\mathbf{q}) = \Pi_{ij}^{\text{sta},(0)} + Q_{ijl}^{\text{sta}} q_l + \mathcal{O}(q^2), \quad \Pi_{ij}^{\text{dyn}}(\mathbf{q}, i\omega_m) = \Pi_{ij}^{\text{dyn},(0)} + Q_{ijl}^{\text{dyn}} q_l + \mathcal{O}(q^2), \quad (\text{S21})$$

with

$$Q_{ijl}^{\text{sta}} = \lim_{\mathbf{q} \rightarrow 0} \frac{\Pi_{ij}^{\text{sta}}(\mathbf{q}) - \Pi_{ij}^{\text{sta}}(0)}{q_l}, \quad Q_{ijl}^{\text{dyn}} = \lim_{\mathbf{q} \rightarrow 0} \frac{\Pi_{ij}^{\text{dyn}}(\mathbf{q}) - \Pi_{ij}^{\text{dyn}}(0)}{q_l}. \quad (\text{S22})$$

The intra-band contribution to  $\Pi_{ij}^{\text{sta},(0)}$  is

$$\begin{aligned}\Pi_{ij}^{\text{sta},(0),\text{intra}} &= \frac{1}{2V} \frac{e^2}{\hbar^2} \sum_{\mathbf{k},\nu} \langle \phi_{\nu,\mathbf{k}} | \partial_{k_i k_j}^2 H_0(\mathbf{k}) \left[ \frac{\epsilon_{\nu,\mathbf{k}} + \xi_{\nu,\mathbf{k}}}{\epsilon_{\nu,\mathbf{k}}} f(\epsilon_{\nu,\mathbf{k}}) + \frac{\epsilon_{\nu,\mathbf{k}} - \xi_{\nu,\mathbf{k}}}{\epsilon_{\nu,\mathbf{k}}} f(-\epsilon_{\nu,\mathbf{k}}) \right] \\ &\quad + \frac{1}{V} \frac{e^2}{\hbar^2} \sum_{\mathbf{k},\nu} \langle \phi_{\nu,\mathbf{k}} | \partial_{k_i} H_0(\mathbf{k}) | \phi_{\nu,\mathbf{k}} \rangle \langle \phi_{\nu,\mathbf{k}} | \partial_{k_j} H_0(\mathbf{k}) | \phi_{\nu,\mathbf{k}} \rangle \frac{df(\epsilon_{\nu,\mathbf{k}})}{d\epsilon_{\nu,\mathbf{k}}} \\ &\approx \frac{1}{V} \frac{e^2}{\hbar^2} \sum_{\mathbf{k},\nu} \left[ \langle \phi_{\nu,\mathbf{k}} | \partial_{k_i k_j}^2 H_0(\mathbf{k}) | \phi_{\nu,\mathbf{k}} \rangle f(\xi_{\nu,\mathbf{k}}) + \langle \phi_{\nu,\mathbf{k}} | \partial_{k_i} H_0(\mathbf{k}) | \phi_{\nu,\mathbf{k}} \rangle \langle \phi_{\nu,\mathbf{k}} | \partial_{k_j} H_0(\mathbf{k}) | \phi_{\nu,\mathbf{k}} \rangle \frac{df(\epsilon_{\nu,\mathbf{k}})}{d\epsilon_{\nu,\mathbf{k}}} \right].\end{aligned}$$

For the inter-band contribution, we assume that the pairing gap  $|\Delta_{\nu,\mathbf{k}}|$  is much smaller than the inversion symmetry breaking induced band splitting, so the inter-band term can be approximated by that in the normal metal phase with  $\Delta_{\nu,\mathbf{k}} = 0$

$$\begin{aligned}\Pi_{ij}^{\text{sta},(0),\text{inter}} &= -\frac{1}{2V} \frac{e^2}{\hbar^2} \sum_{\mathbf{k},\nu \neq \nu'} \left[ \left( 1 - \frac{\xi_{\nu,\mathbf{k}} \xi_{\nu',\mathbf{k}} + \Delta_{\nu,\mathbf{k}} \Delta_{\nu',\mathbf{k}}^*}{\epsilon_{\nu',\mathbf{k}} \epsilon_{\nu,\mathbf{k}}} \right) \frac{1 - f(\epsilon_{\nu',\mathbf{k}}) - f(\epsilon_{\nu,\mathbf{k}})}{\epsilon_{\nu',\mathbf{k}} + \epsilon_{\nu,\mathbf{k}}} \right. \\ &\quad \left. - \left( 1 + \frac{\xi_{\nu,\mathbf{k}} \xi_{\nu',\mathbf{k}} + \Delta_{\nu,\mathbf{k}} \Delta_{\nu',\mathbf{k}}^*}{\epsilon_{\nu',\mathbf{k}} \epsilon_{\nu,\mathbf{k}}} \right) \frac{f(\epsilon_{\nu',\mathbf{k}}) - f(\epsilon_{\nu,\mathbf{k}})}{\epsilon_{\nu',\mathbf{k}} - \epsilon_{\nu,\mathbf{k}}} \right] \langle \phi_{\nu,\mathbf{k}} | \partial_{k_i} H_0(\mathbf{k}) | \phi_{\nu',\mathbf{k}} \rangle \langle \phi_{\nu',\mathbf{k}} | \partial_{k_j} H_0(\mathbf{k}) | \phi_{\nu,\mathbf{k}} \rangle \\ &\approx \frac{1}{V} \frac{e^2}{\hbar^2} \sum_{\mathbf{k},\nu \neq \nu'} \frac{f(\xi_{\nu',\mathbf{k}}) - f(\xi_{\nu,\mathbf{k}})}{\xi_{\nu',\mathbf{k}} - \xi_{\nu,\mathbf{k}}} \langle \phi_{\nu,\mathbf{k}} | \partial_{k_i} H_0(\mathbf{k}) | \phi_{\nu',\mathbf{k}} \rangle \langle \phi_{\nu',\mathbf{k}} | \partial_{k_j} H_0(\mathbf{k}) | \phi_{\nu,\mathbf{k}} \rangle.\end{aligned}\quad (\text{S23})$$

We also know from the gauge invariance that

$$\begin{aligned}&\frac{1}{V} \frac{e^2}{\hbar^2} \sum_{\mathbf{k},\nu \neq \nu'} \frac{f(\xi_{\nu',\mathbf{k}}) - f(\xi_{\nu,\mathbf{k}})}{\xi_{\nu',\mathbf{k}} - \xi_{\nu,\mathbf{k}}} \langle \phi_{\nu,\mathbf{k}} | \partial_{k_i} H_0(\mathbf{k}) | \phi_{\nu',\mathbf{k}} \rangle \langle \phi_{\nu',\mathbf{k}} | \partial_{k_j} H_0(\mathbf{k}) | \phi_{\nu,\mathbf{k}} \rangle \\ &= -\frac{1}{V} \frac{e^2}{\hbar^2} \sum_{\mathbf{k},\nu} \left[ \langle \phi_{\nu,\mathbf{k}} | \partial_{k_i} H_0(\mathbf{k}) | \phi_{\nu,\mathbf{k}} \rangle \langle \phi_{\nu,\mathbf{k}} | \partial_{k_j} H_0(\mathbf{k}) | \phi_{\nu,\mathbf{k}} \rangle \frac{df(\xi_{\nu,\mathbf{k}})}{d\xi_{\nu,\mathbf{k}}} + \langle \phi_{\nu,\mathbf{k}} | \partial_{k_i k_j}^2 H_0(\mathbf{k}) | \phi_{\nu,\mathbf{k}} \rangle f(\xi_{\nu,\mathbf{k}}) \right],\end{aligned}\quad (\text{S24})$$

so eventually we obtain the  $\Pi_{ij}^{\text{sta},(0)}$

$$\begin{aligned}\Pi_{ij}^{\text{sta},(0)} &= \Pi_{ij}^{\text{sta},(0),\text{intra}} + \Pi_{ij}^{\text{sta},(0),\text{inter}} \\ &= \frac{1}{V} \frac{e^2}{\hbar^2} \sum_{\nu,\mathbf{k}} \langle \phi_{\nu,\mathbf{k}} | \partial_{k_i} H_0(\mathbf{k}) | \phi_{\nu,\mathbf{k}} \rangle \langle \phi_{\nu,\mathbf{k}} | \partial_{k_j} H_0(\mathbf{k}) | \phi_{\nu,\mathbf{k}} \rangle \left[ \frac{df(\epsilon_{\nu,\mathbf{k}})}{d\epsilon_{\nu,\mathbf{k}}} - \frac{df(\xi_{\nu,\mathbf{k}})}{d\xi_{\nu,\mathbf{k}}} \right] \\ &= \frac{e^2}{\hbar^2} \frac{1}{(2\pi)^d} \int_{\text{BZ}} d\mathbf{k} \sum_{\nu} v_{\nu,\mathbf{k},i} v_{\nu,\mathbf{k},j} \left[ \frac{df(\epsilon_{\nu,\mathbf{k}})}{d\epsilon_{\nu,\mathbf{k}}} - \frac{df(\xi_{\nu,\mathbf{k}})}{d\xi_{\nu,\mathbf{k}}} \right],\end{aligned}\quad (\text{S25})$$

with the group velocity  $\mathbf{v}_{\nu,\mathbf{k}} = \nabla_{\mathbf{k}} \xi_{\nu,\mathbf{k}} = \langle \phi_{\nu,\mathbf{k}} | \nabla_{\mathbf{k}} H_0(\mathbf{k}) | \phi_{\nu,\mathbf{k}} \rangle$ . For the term  $\Pi_{ij}^{\text{dyn},(0)}$  that is  $i\omega_m$  dependent, we consider the dominant intra-band contribution and take the analytic continuation  $i\omega_m \rightarrow \hbar\omega + i\hbar\tau^{-1}$  to get

$$\Pi_{ij}^{\text{dyn},(0)} = \frac{e^2}{\hbar^2} \frac{i\omega\tau}{1 - i\omega\tau} \sum_{\nu} \int_{\text{BZ}} v_{\nu,\mathbf{k},i} v_{\nu,\mathbf{k},j} \frac{df(\epsilon_{\nu,\mathbf{k}})}{d\epsilon_{\nu,\mathbf{k}}} \frac{d\mathbf{k}}{(2\pi)^d}.\quad (\text{S26})$$

The intra-band contribution to  $Q_{ijl}^{\text{sta}}$  is [S2, S3]

$$Q_{ijl}^{\text{sta},\text{intra}} = \frac{i}{V} \frac{e}{\hbar} \sum_{\nu,\mathbf{k}} \frac{df(\epsilon_{\nu,\mathbf{k}})}{d\epsilon_{\nu,\mathbf{k}}} \left( \partial_{k_i} \xi_{\nu,\mathbf{k}} \epsilon_{dlj} m_{\nu,\mathbf{k},d} - \partial_{k_j} \xi_{\nu,\mathbf{k}} \epsilon_{dli} m_{\nu,\mathbf{k},d} \right),$$

with  $\mathbf{m}_{\nu,\mathbf{k}} = \frac{ie}{2\hbar} \langle \partial_{\mathbf{k}} \phi_{\nu,\mathbf{k}} | \times [H_0(\mathbf{k}) - \xi_{\nu,\mathbf{k}}] | \partial_{\mathbf{k}} \phi_{\nu,\mathbf{k}} \rangle$  the orbital magnetic moment. For the inter-band contribution, given the pairing gap  $|\Delta_{\nu,\mathbf{k}}|$  much smaller than the band splitting, it is also approximated by that in the normal metal phase similar to Eq. S23. Since we know the summation of intra-band and inter-band static term in the normal metal

phase gives  $Q_{ijl}^{\text{sta}} = \frac{e^2}{\hbar^2} \int_{\text{BZ}} \frac{d\mathbf{k}}{(2\pi)^d} \sum_{\nu} 2f(\epsilon_{\nu,\mathbf{k}}) \nabla_{\mathbf{k}} \cdot (\epsilon_{\nu,\mathbf{k}} \boldsymbol{\Omega}_{\nu,\mathbf{k}})$ , which is confirmed to be zero [S2, S3]. As a result, the inter-band contribution to  $Q_{ijl}^{\text{sta}}$  is

$$Q_{ijl}^{\text{sta,inter}} = -\frac{i}{V} \frac{e}{\hbar} \sum_{\nu,\mathbf{k}} \frac{df(\xi_{\nu,\mathbf{k}})}{d\xi_{\nu,\mathbf{k}}} (\partial_{k_i} \xi_{\nu,\mathbf{k}} \epsilon_{dlj} m_{\nu,\mathbf{k},d} - \partial_{k_j} \xi_{\nu,\mathbf{k}} \epsilon_{dli} m_{\nu,\mathbf{k},d}). \quad (\text{S27})$$

For the dynamic part  $Q_{ijl}^{\text{dyn}}$ , we consider the dominant intra-band term and use the analytical continuation  $i\omega_m \rightarrow \hbar\omega + i\hbar\tau^{-1}$  as well, and then we can obtain

$$Q_{ijl}^{\text{dyn}} = -\frac{1}{V} \frac{e}{\hbar} \frac{\omega\tau}{1-i\omega\tau} \sum_{\nu,\mathbf{k}} \frac{df(\epsilon_{\nu,\mathbf{k}})}{d\epsilon_{\nu,\mathbf{k}}} (\partial_{k_i} \xi_{\nu,\mathbf{k}} \epsilon_{dlj} m_{\nu,\mathbf{k},d} - \partial_{k_j} \xi_{\nu,\mathbf{k}} \epsilon_{dli} m_{\nu,\mathbf{k},d}). \quad (\text{S28})$$

Eventually, the polarization tensor  $\Pi_{ij}(\mathbf{q}, \omega)$  becomes

$$\begin{aligned} \Pi_{ij}(\mathbf{q}, \omega) &\approx \Pi_{ij}^{\text{sta,(0)}} + Q_{ijl}^{\text{sta}} q_l + \Pi_{ij}^{\text{dyn,(0)}} + Q_{ijl}^{\text{dyn}} q_l \\ &= \frac{e^2}{\hbar^2} \int_{\text{BZ}} \frac{d\mathbf{k}}{(2\pi)^d} \sum_{\nu} v_{\nu,\mathbf{k},i} v_{\nu,\mathbf{k},j} \left[ \frac{df(\epsilon_{\nu,\mathbf{k}})}{d\epsilon_{\nu,\mathbf{k}}} - \frac{df(\xi_{\nu,\mathbf{k}})}{d\xi_{\nu,\mathbf{k}}} \right] + \frac{e^2}{\hbar^2} \frac{i\omega\tau}{1-i\omega\tau} \int_{\text{BZ}} \frac{d\mathbf{k}}{(2\pi)^d} \sum_{\nu} v_{\nu,\mathbf{k},i} v_{\nu,\mathbf{k},j} \frac{df(\epsilon_{\nu,\mathbf{k}})}{d\epsilon_{\nu,\mathbf{k}}} \\ &\quad + \frac{i}{V} \frac{e}{\hbar} \sum_{\nu,\mathbf{k}} (v_{\nu,\mathbf{k},i} \epsilon_{dlj} m_{\nu,\mathbf{k},d} - v_{\nu,\mathbf{k},j} \epsilon_{dli} m_{\nu,\mathbf{k},d}) \left[ \frac{df(\epsilon_{\nu,\mathbf{k}})}{d\epsilon_{\nu,\mathbf{k}}} - \frac{df(\xi_{\nu,\mathbf{k}})}{d\xi_{\nu,\mathbf{k}}} \right] \\ &\quad - \frac{1}{V} \frac{e}{\hbar} \frac{\omega\tau}{1-i\omega\tau} \sum_{\nu,\mathbf{k}} (v_{\nu,\mathbf{k},i} \epsilon_{dlj} m_{\nu,\mathbf{k},d} - v_{\nu,\mathbf{k},j} \epsilon_{dli} m_{\nu,\mathbf{k},d}) \frac{df(\epsilon_{\nu,\mathbf{k}})}{d\epsilon_{\nu,\mathbf{k}}}. \end{aligned} \quad (\text{S29})$$

From Eq. S15 we can then obtain the current density to be

$$J_i = -\frac{\partial \Delta F}{\partial A_i} = -\frac{e^2}{\hbar^2} \sum_{\nu} \int_{\text{BZ}} v_{\nu,\mathbf{k},i} v_{\nu,\mathbf{k},j} \left\{ \frac{\tau}{1-i\omega\tau} \frac{df(\epsilon_{\nu,\mathbf{k}})}{d\epsilon_{\nu,\mathbf{k}}} E_j + \left[ \frac{df(\epsilon_{\nu,\mathbf{k}})}{d\epsilon_{\nu,\mathbf{k}}} - \frac{df(\xi_{\nu,\mathbf{k}})}{d\xi_{\nu,\mathbf{k}}} \right] A_j \right\}, \quad (\text{S30})$$

Interestingly, we notice that the  $Q_{ijl}^{\text{sta}}$  and  $Q_{ijl}^{\text{dyn}}$  related free energy density can be further simplified as

$$\begin{aligned} \Delta F_Q &= -\frac{i}{V} \frac{e}{\hbar} \sum_{\nu,\mathbf{k},\mathbf{q},m} \frac{1}{2} A_i(-\mathbf{q}, -i\omega_m) \left[ \frac{df(\xi_{\nu,\mathbf{k}})}{d\xi_{\nu,\mathbf{k}}} - \frac{df(\epsilon_{\nu,\mathbf{k}})}{d\epsilon_{\nu,\mathbf{k}}} \right] (v_{\nu,\mathbf{k},i} m_{\nu,\mathbf{k},d} \epsilon_{dlj} - v_{\nu,\mathbf{k},j} m_{\nu,\mathbf{k},d} \epsilon_{dli}) q_l A_j(\mathbf{q}, i\omega_m) \\ &= -\frac{1}{2} \sum_{\nu,\mathbf{q},\omega} B_i(-\mathbf{q}, -\omega) \frac{e}{\hbar} \int_{\text{BZ}} \frac{d\mathbf{k}}{(2\pi)^d} m_{\nu,\mathbf{k},i} v_{\nu,\mathbf{k},j} \left[ \frac{df(\xi_{\nu,\mathbf{k}})}{d\xi_{\nu,\mathbf{k}}} - \frac{df(\epsilon_{\nu,\mathbf{k}})}{d\epsilon_{\nu,\mathbf{k}}} \right] A_j(\mathbf{q}, \omega) \\ &\quad + \frac{1}{2} \sum_{\nu,\mathbf{q},\omega} B_i(-\mathbf{q}, -\omega) \frac{e}{\hbar} \frac{i\omega\tau}{1-i\omega\tau} \int_{\text{BZ}} \frac{d\mathbf{k}}{(2\pi)^d} m_{\nu,\mathbf{k},i} v_{\nu,\mathbf{k},j} \frac{df(\epsilon_{\nu,\mathbf{k}})}{d\epsilon_{\nu,\mathbf{k}}} A_j(\mathbf{q}, \omega) \\ &\quad - \frac{1}{2} \sum_{\nu,\mathbf{q},\omega} A_i(-\mathbf{q}, \omega) \frac{e}{\hbar} \int_{\text{BZ}} \frac{d\mathbf{k}}{(2\pi)^d} v_{\nu,\mathbf{k},i} m_{\nu,\mathbf{k},j} \left[ \frac{df(\xi_{\nu,\mathbf{k}})}{d\xi_{\nu,\mathbf{k}}} - \frac{df(\epsilon_{\nu,\mathbf{k}})}{d\epsilon_{\nu,\mathbf{k}}} \right] B_j(\mathbf{q}, \omega) \\ &\quad + \frac{1}{2} \sum_{\nu,\mathbf{q},\omega} A_i(-\mathbf{q}, -\omega) \frac{e}{\hbar} \frac{i\omega\tau}{1-i\omega\tau} \int_{\text{BZ}} \frac{d\mathbf{k}}{(2\pi)^d} v_{\nu,\mathbf{k},i} m_{\nu,\mathbf{k},j} \frac{df(\epsilon_{\nu,\mathbf{k}})}{d\epsilon_{\nu,\mathbf{k}}} B_j(\mathbf{q}, \omega). \end{aligned} \quad (\text{S31})$$

Eventually, we get the current induced orbital magnetization to be

$$m_i = -\frac{\partial \Delta F}{\partial B_i} = -\frac{e}{\hbar} \sum_{\nu} \int_{\text{BZ}} m_{\nu,\mathbf{k},i} v_{\nu,\mathbf{k},j} \left\{ \frac{\tau}{1-i\omega\tau} \frac{df(\epsilon_{\nu,\mathbf{k}})}{d\epsilon_{\nu,\mathbf{k}}} E_j + \left[ \frac{df(\epsilon_{\nu,\mathbf{k}})}{d\epsilon_{\nu,\mathbf{k}}} - \frac{df(\xi_{\nu,\mathbf{k}})}{d\xi_{\nu,\mathbf{k}}} \right] A_j \right\}. \quad (\text{S32})$$

Here the electric field has been expressed in terms of the vector gauge potential as  $\mathbf{E} = i\omega \mathbf{A}$ .

### Spin Magnetoelectric Susceptibility Calculation

The spin magnetoelectric susceptibility  $T_{ij}^s$  is calculated to be

$$T_{ij}^s = -\frac{1}{\beta V} \sum_{\mathbf{k}, n, \nu, \nu'} \frac{\left( \omega_n^2 + \omega_n \omega_m - \xi_{\nu,\mathbf{k}} \xi_{\nu',\mathbf{k}} - \Delta_{\nu,\mathbf{k}} \Delta_{\nu',\mathbf{k}}^* \right) \langle \phi_{\nu,\mathbf{k}} | \frac{1}{2} \mu_B \sigma_i | \phi_{\nu',\mathbf{k}} \rangle \langle \phi_{\nu',\mathbf{k}} | \frac{e}{\hbar} \partial_{k_j} H_0(\mathbf{k}) | \phi_{\nu,\mathbf{k}} \rangle}{\left[ \omega_n^2 + \xi_{\nu,\mathbf{k}}^2 + \Delta_{\nu,\mathbf{k}}^* \Delta_{\nu,\mathbf{k}} \right] \left[ (\omega_n + \omega_m)^2 + \xi_{\nu',\mathbf{k}}^2 + \Delta_{\nu',\mathbf{k}}^* \Delta_{\nu',\mathbf{k}} \right]}. \quad (\text{S33})$$

We further sum over the Matsubara frequency and decompose the spin magnetoelectric susceptibility into the static ( $i\omega_m = 0$ ) and dynamic ( $i\omega_m \neq 0$ ) part as

$$T_{ij}^s = T_{ij}^{s,\text{sta}} + T_{ij}^{s,\text{dyn}}(i\omega_m), \quad (\text{S34})$$

with

$$T_{ij}^{s,\text{sta}} = -\frac{1}{V} \sum_{\mathbf{k}, \nu, \nu'} \left[ \frac{1}{2} \left( 1 - \frac{\xi_{\nu, \mathbf{k}} \xi_{\nu', \mathbf{k}} + \Delta_{\nu, \mathbf{k}} \Delta_{\nu', \mathbf{k}}^*}{\epsilon_{\nu', \mathbf{k}} \epsilon_{\nu, \mathbf{k}}} \right) \frac{1 - f(\epsilon_{\nu', \mathbf{k}}) - f(\epsilon_{\nu, \mathbf{k}})}{\epsilon_{\nu', \mathbf{k}} + \epsilon_{\nu, \mathbf{k}}} - \frac{1}{2} \left( 1 + \frac{\xi_{\nu, \mathbf{k}} \xi_{\nu', \mathbf{k}} + \Delta_{\nu, \mathbf{k}} \Delta_{\nu', \mathbf{k}}^*}{\epsilon_{\nu', \mathbf{k}} \epsilon_{\nu, \mathbf{k}}} \right) \frac{f(\epsilon_{\nu', \mathbf{k}}) - f(\epsilon_{\nu, \mathbf{k}})}{\epsilon_{\nu', \mathbf{k}} - \epsilon_{\nu, \mathbf{k}}} \right] \langle \phi_{\nu, \mathbf{k}} | \frac{1}{2} \mu_b g \sigma_i | \phi_{\nu', \mathbf{k}} \rangle \langle \phi_{\nu', \mathbf{k}} | \frac{e}{\hbar} \partial_{k_j} H_0(\mathbf{k}) | \phi_{\nu, \mathbf{k}} \rangle, \quad (\text{S35})$$

and

$$T_{ij}^{s,\text{dyn}}(i\omega_m) = -\frac{1}{V} \sum_{\mathbf{k}, \nu, \nu'} \left\{ \frac{1}{4} \left( 1 - \frac{\xi_{\nu, \mathbf{k}} \xi_{\nu', \mathbf{k}} + \Delta_{\nu, \mathbf{k}} \Delta_{\nu', \mathbf{k}}^*}{\epsilon_{\nu, \mathbf{k}} \epsilon_{\nu', \mathbf{k}}} \right) \left[ \frac{i\omega_m}{i\omega_m + \epsilon_{\nu', \mathbf{k}} + \epsilon_{\nu, \mathbf{k}}} + \frac{i\omega_m}{i\omega_m - (\epsilon_{\nu', \mathbf{k}} + \epsilon_{\nu, \mathbf{k}})} \right] \frac{1 - f(\epsilon_{\nu', \mathbf{k}}) - f(\epsilon_{\nu, \mathbf{k}})}{\epsilon_{\nu', \mathbf{k}} + \epsilon_{\nu, \mathbf{k}}} \right. \\ \left. \frac{1}{4} \left( 1 + \frac{\xi_{\nu, \mathbf{k}} \xi_{\nu', \mathbf{k}} + \Delta_{\nu, \mathbf{k}} \Delta_{\nu', \mathbf{k}}^*}{\epsilon_{\nu', \mathbf{k}} \epsilon_{\nu, \mathbf{k}}} \right) \left[ \frac{i\omega_m}{i\omega_m - (\epsilon_{\nu', \mathbf{k}} - \epsilon_{\nu, \mathbf{k}})} + \frac{i\omega_m}{i\omega_m + \epsilon_{\nu', \mathbf{k}} - \epsilon_{\nu, \mathbf{k}}} \right] \frac{f(\epsilon_{\nu', \mathbf{k}}) - f(\epsilon_{\nu, \mathbf{k}})}{\epsilon_{\nu', \mathbf{k}} - \epsilon_{\nu, \mathbf{k}}} \right\} \langle \phi_{\nu, \mathbf{k}} | \frac{1}{2} \mu_b g \sigma_i | \phi_{\nu', \mathbf{k}} \rangle \langle \phi_{\nu', \mathbf{k}} | \frac{e}{\hbar} \partial_{k_j} H_0(\mathbf{k}) | \phi_{\nu, \mathbf{k}} \rangle. \quad (\text{S36})$$

The intra-band contribution to  $T_{ij}^{s,\text{sta}}$  is

$$T_{ij}^{s,\text{sta},\text{intra}} = \frac{1}{V} \sum_{\mathbf{k}, \nu} \frac{df(\epsilon_{\nu, \mathbf{k}})}{d\epsilon_{\nu, \mathbf{k}}} \langle \phi_{\nu, \mathbf{k}} | \frac{1}{2} \mu_b g \sigma_i | \phi_{\nu, \mathbf{k}} \rangle \langle \phi_{\nu, \mathbf{k}} | \frac{e}{\hbar} \partial_{k_i} H_0(\mathbf{k}) | \phi_{\nu, \mathbf{k}} \rangle. \quad (\text{S37})$$

For the inter-band contribution, similarly, we assume that the pairing gap  $|\Delta_{\nu, \mathbf{k}}|$  is much smaller than the band splitting so that it can be approximated by that in the normal metal phase. We also know that the summation of intra-band and inter-band term in the static limit will vanish, so the inter-band contribution can be written as

$$T_{ij}^{s,\text{sta},\text{inter}} = -\frac{1}{V} \sum_{\mathbf{k}, \nu} \frac{df(\xi_{\nu, \mathbf{k}})}{d\xi_{\nu, \mathbf{k}}} \langle \phi_{\nu, \mathbf{k}} | \frac{1}{2} \mu_b g \sigma_i | \phi_{\nu, \mathbf{k}} \rangle \langle \phi_{\nu, \mathbf{k}} | \frac{e}{\hbar} \partial_{k_j} H_0(\mathbf{k}) | \phi_{\nu, \mathbf{k}} \rangle. \quad (\text{S38})$$

We know that for a Bloch state the spin magnetic moment is  $\mathbf{S}_{\nu, \mathbf{k}} = \langle \phi_{\nu, \mathbf{k}} | \frac{1}{2} \mu_b g \boldsymbol{\sigma} | \phi_{\nu, \mathbf{k}} \rangle$ , so the static part of the spin magnetoelectric susceptibility reads

$$T_{ij}^{s,\text{sta}} = T_{ij}^{s,\text{sta},\text{intra}} + T_{ij}^{s,\text{sta},\text{inter}} \\ = -\frac{e}{\hbar} \int_{\text{BZ}} \frac{d\mathbf{k}}{(2\pi)^d} \sum_{\nu} S_{\nu, \mathbf{k}, i} v_{\nu, \mathbf{k}, j} \left[ \frac{df(\xi_{\nu, \mathbf{k}})}{d\xi_{\nu, \mathbf{k}}} - \frac{df(\epsilon_{\nu, \mathbf{k}})}{d\epsilon_{\nu, \mathbf{k}}} \right]. \quad (\text{S39})$$

The  $\tilde{T}_{ij}^{s,\text{sta}}$  can be obtained similarly following the above procedure

$$\tilde{T}_{ij}^{s,\text{sta}} = -\frac{e}{\hbar} \int_{\text{BZ}} \frac{d\mathbf{k}}{(2\pi)^d} \sum_{\nu} v_{\nu, \mathbf{k}, i} S_{\nu, \mathbf{k}, j} \left[ \frac{df(\xi_{\nu, \mathbf{k}})}{d\xi_{\nu, \mathbf{k}}} - \frac{df(\epsilon_{\nu, \mathbf{k}})}{d\epsilon_{\nu, \mathbf{k}}} \right]. \quad (\text{S40})$$

For the dynamic part that is  $i\omega_m$  dependent, we consider the dominant intra-band contribution and obtain

$$T_{ij}^{s,\text{dyn}}(i\omega_m) = \frac{i\omega\tau}{1 - i\omega\tau} \frac{e}{\hbar} \int_{\text{BZ}} \frac{d\mathbf{k}}{(2\pi)^d} \sum_{\nu} S_{\nu, \mathbf{k}, i} v_{\nu, \mathbf{k}, j} \frac{df(\epsilon_{\nu, \mathbf{k}})}{d\epsilon_{\nu, \mathbf{k}}}. \quad (\text{S41})$$

The  $\tilde{T}_{ij}^{s,\text{dyn}}(i\omega_m)$  can be obtained similarly following the above procedure as well

$$\tilde{T}_{ij}^{s,\text{dyn}}(i\omega_m) = \frac{i\omega\tau}{1 - i\omega\tau} \frac{e}{\hbar} \int_{\text{BZ}} \frac{d\mathbf{k}}{(2\pi)^d} \sum_{\nu} v_{\nu, \mathbf{k}, i} S_{\nu, \mathbf{k}, j} \frac{df(\epsilon_{\nu, \mathbf{k}})}{d\epsilon_{\nu, \mathbf{k}}}. \quad (\text{S42})$$

Eventually, we get the spin magnetoelectric susceptibility as

$$T_{ij}^s = -\frac{e}{\hbar} \int_{\text{BZ}} \frac{d\mathbf{k}}{(2\pi)^d} \sum_{\nu} S_{\nu, \mathbf{k}, i} v_{\nu, \mathbf{k}, j} \left[ \frac{df(\xi_{\nu, \mathbf{k}})}{d\xi_{\nu, \mathbf{k}}} - \frac{df(\epsilon_{\nu, \mathbf{k}})}{d\epsilon_{\nu, \mathbf{k}}} \right] + \frac{i\omega\tau}{1 - i\omega\tau} \frac{e}{\hbar} \int_{\text{BZ}} \frac{d\mathbf{k}}{(2\pi)^d} \sum_{\nu} S_{\nu, \mathbf{k}, i} v_{\nu, \mathbf{k}, j} \frac{df(\epsilon_{\nu, \mathbf{k}})}{d\epsilon_{\nu, \mathbf{k}}}, \quad (\text{S43})$$

$$\tilde{T}_{ij}^s = -\frac{e}{\hbar} \int_{\text{BZ}} \frac{d\mathbf{k}}{(2\pi)^d} \sum_{\nu} v_{\nu, \mathbf{k}, i} S_{\nu, \mathbf{k}, j} \left[ \frac{df(\xi_{\nu, \mathbf{k}})}{d\xi_{\nu, \mathbf{k}}} - \frac{df(\epsilon_{\nu, \mathbf{k}})}{d\epsilon_{\nu, \mathbf{k}}} \right] + \frac{i\omega\tau}{1 - i\omega\tau} \frac{e}{\hbar} \int_{\text{BZ}} \frac{d\mathbf{k}}{(2\pi)^d} \sum_{\nu} v_{\nu, \mathbf{k}, i} S_{\nu, \mathbf{k}, j} \frac{df(\epsilon_{\nu, \mathbf{k}})}{d\epsilon_{\nu, \mathbf{k}}}. \quad (\text{S44})$$

### Current Induced Total Magnetization

Now it is ready to write down the total magnetization

$$M_i = -\frac{\partial \Delta F}{\partial B_i} = -\frac{e}{\hbar} \int_{\text{BZ}} \frac{d\mathbf{k}}{(2\pi)^d} \sum_{\nu} M_{\nu, \mathbf{k}, i} v_{\nu, \mathbf{k}, j} \left\{ \frac{\tau}{1 - i\omega\tau} \frac{df(\epsilon_{\nu, \mathbf{k}})}{d\epsilon_{\nu, \mathbf{k}}} E_j + \left[ \frac{df(\epsilon_{\nu, \mathbf{k}})}{d\epsilon_{\nu, \mathbf{k}}} - \frac{df(\xi_{\nu, \mathbf{k}})}{d\xi_{\nu, \mathbf{k}}} \right] A_j \right\}, \quad (\text{S45})$$

which is induced by the current density

$$J_i = -\frac{\partial \Delta F}{\partial A_i} = -\frac{e^2}{\hbar^2} \int_{\text{BZ}} \frac{d\mathbf{k}}{(2\pi)^d} \sum_{\nu} v_{\nu, \mathbf{k}, i} v_{\nu, \mathbf{k}, j} \left\{ \frac{\tau}{1 - i\omega\tau} \frac{df(\epsilon_{\nu, \mathbf{k}})}{d\epsilon_{\nu, \mathbf{k}}} E_j + \left[ \frac{df(\epsilon_{\nu, \mathbf{k}})}{d\epsilon_{\nu, \mathbf{k}}} - \frac{df(\xi_{\nu, \mathbf{k}})}{d\xi_{\nu, \mathbf{k}}} \right] A_j \right\}. \quad (\text{S46})$$

The total magnetic moment  $\mathbf{M}_{\nu, \mathbf{k}} = \mathbf{m}_{\nu, \mathbf{k}} + \mathbf{S}_{\nu, \mathbf{k}}$  includes both the orbital magnetic moment  $\mathbf{m}_{\nu, \mathbf{k}}$  and the spin magnetic moment  $\mathbf{S}_{\nu, \mathbf{k}}$ . As a result, at given current density  $\mathbf{J}$ , the induced magnetization becomes  $M_i = \alpha_{ik} J_k$ , where  $\alpha_{ik}$  can be directly calculated at zero temperature limit and above the critical temperature  $T_c$ . At the critical temperature  $T_c$ , the L'Hospital rule is used to get the  $\alpha_{ik}$  there.

### CONTINUUM MODEL FOR THE TWISTED BILAYER GRAPHENE

In the monolayer graphene, the primitive lattice vectors and the corresponding reciprocal primitive lattice vectors are

$$\mathbf{a}_1^0 = \sqrt{3} \left( \frac{1}{2}, \frac{\sqrt{3}}{2} \right) d, \quad \mathbf{a}_2^0 = \sqrt{3} \left( -\frac{1}{2}, \frac{\sqrt{3}}{2} \right) d, \quad (\text{S47})$$

$$\mathbf{b}_1^0 = \frac{4\pi}{3d} \left( \frac{\sqrt{3}}{2}, \frac{1}{2} \right), \quad \mathbf{b}_2^0 = \frac{4\pi}{3d} \left( -\frac{\sqrt{3}}{2}, \frac{1}{2} \right), \quad (\text{S48})$$

with  $d = 1.42\text{\AA}$ . We also define the vector that links the origin of the unit cell to its respective sublattice  $\alpha = A, B$  atom to be  $\boldsymbol{\delta}_A = \mathbf{0}$ ,  $\boldsymbol{\delta}_B = d(0, 1)$ . The Dirac points localize at the Brillouin zone corner  $\mathbf{K}_{\pm} = \frac{4\pi}{3d} \left( \frac{\sqrt{3}}{2}, \frac{1}{2} \right)$ . Given the uniaxial strain tensor  $\boldsymbol{\mathcal{E}}$  along the zig-zag direction of one graphene layer as

$$\boldsymbol{\mathcal{E}} = \varepsilon \begin{pmatrix} -1 & 0 \\ 0 & \nu_{\text{poi}} \end{pmatrix}, \quad (\text{S49})$$

with the Poison's ratio  $\nu_{\text{poi}} = 0.165$ , we know that the uniaxial strain will deform both the real and reciprocal space as

$$\tilde{\mathbf{r}} = (1 + \boldsymbol{\mathcal{E}}) \mathbf{r}, \quad \tilde{\mathbf{k}} = (1 - \boldsymbol{\mathcal{E}}^T) \mathbf{k}_0. \quad (\text{S50})$$

As a result, the strain changes the position of the Dirac points in the reciprocal space to be

$$\tilde{\mathbf{K}}_{\eta} = (1 - \boldsymbol{\mathcal{E}}^T) \mathbf{K}_{\eta} - \eta \mathbf{A}_{\text{strain}}, \quad (\text{S51})$$

with the valley index  $\eta = \pm 1$  and the strain induced effective gauge field  $\mathbf{A}_{\text{strain}} = \frac{\beta}{d} (\mathcal{E}_{xx} - \mathcal{E}_{yy}, -2\mathcal{E}_{xy})$ ,  $\beta = 1.57$ . The Hamiltonian for the bottom layer graphene at the valley  $\eta$  becomes

$$\tilde{\mathcal{H}}_{\text{b}} = \sum_{\mathbf{k}, s, \eta} c_{\text{b}, s, \eta}^{\dagger}(\mathbf{k}) h_{\text{b}, \eta}(\mathbf{k}) c_{\text{b}, s, \eta}(\mathbf{k}) = \sum_{\mathbf{k}, s, \eta} c_{\text{b}, s, \eta}^{\dagger} \left[ \eta \hbar v_{\text{F}} \hat{\mathbf{R}}_{-\frac{\theta}{2}} \left( 1 + \boldsymbol{\mathcal{E}}^T \right) (\mathbf{k} + \eta \mathbf{A}_{\text{strain}}) \cdot \boldsymbol{\sigma} + \Delta \sigma_z \right] c_{\text{b}, s, \eta}(\mathbf{k}), \quad (\text{S52})$$

with the spin index  $s = \uparrow, \downarrow$ , the rotation matrix  $\hat{\mathbf{R}}_{-\frac{\theta}{2}} = \cos \frac{\theta}{2} + i\sigma_y \sin \frac{\theta}{2}$ , the momentum  $\mathbf{k} = \mathbf{k} - (1 - \boldsymbol{\mathcal{E}}^T) \mathbf{K}_{\eta}$ . The top layer graphene has the Hamiltonian

$$\mathcal{H}_{\text{t}} = \sum_{\mathbf{k}, s, \eta} c_{\text{t}, s, \eta}^{\dagger}(\mathbf{k}) h_{\text{t}, \eta}(\mathbf{k}) c_{\text{t}, s, \eta}(\mathbf{k}) = \sum_{\mathbf{k}, s, \eta} c_{\text{t}, s, \eta}^{\dagger}(\mathbf{k}) \eta \hbar v_{\text{F}} \hat{\mathbf{R}}_{\frac{\theta}{2}} \mathbf{k} \cdot \boldsymbol{\sigma} c_{\text{t}, s, \eta}(\mathbf{k}). \quad (\text{S53})$$

Then we consider the tunneling matrix element from the bottom layer to the top layer as [S4–S6]

$$\begin{aligned} \tilde{T}_{\hat{\mathbf{R}}_{-\frac{\theta}{2}}\tilde{\mathbf{K}}_{\eta}+\mathbf{k},\hat{\mathbf{R}}_{\frac{\theta}{2}}\mathbf{K}_{\eta}+\mathbf{k}'}^{\alpha,\beta} = & \frac{1}{3}t_{\perp} \left[ \delta_{\hat{\mathbf{R}}_{-\frac{\theta}{2}}\tilde{\mathbf{K}}_{\eta}+\mathbf{k},\hat{\mathbf{R}}_{\frac{\theta}{2}}\mathbf{K}_{\eta}+\mathbf{k}'} + e^{i\tilde{\mathbf{b}}_2\cdot(\tilde{\delta}_{\alpha}-\tilde{\delta}_{\beta})}\delta_{\hat{\mathbf{R}}_{-\frac{\theta}{2}}(\tilde{\mathbf{K}}_{\eta}+\tilde{\mathbf{b}}_2)+\mathbf{k},\hat{\mathbf{R}}_{\frac{\theta}{2}}(\mathbf{K}_{\eta}+\mathbf{b}_2)+\mathbf{k}'} \right. \\ & \left. + e^{-i\tilde{\mathbf{b}}_1\cdot(\tilde{\delta}_{\alpha}-\tilde{\delta}_{\beta})}\delta_{\hat{\mathbf{R}}_{-\frac{\theta}{2}}(\tilde{\mathbf{K}}_{\eta}-\tilde{\mathbf{b}}_1)+\mathbf{k},\hat{\mathbf{R}}_{\frac{\theta}{2}}(\mathbf{K}_{\eta}-\mathbf{b}_1)+\mathbf{k}'} \right], \end{aligned} \quad (\text{S54})$$

so the strain deformed interlayer Hamiltonian becomes

$$\tilde{\mathcal{H}}_{\text{int}} = \sum_{\mathbf{k},s,\eta} c_{\text{b},s,\eta}^{\dagger}(\mathbf{k}) \left[ \tilde{T}_{\eta\tilde{\mathbf{k}}_{\text{b}}} \delta_{\mathbf{k}'-\mathbf{k},\eta\tilde{\mathbf{k}}_{\text{b}}} + \tilde{T}_{\eta\tilde{\mathbf{k}}_{\text{tr}}} \delta_{\mathbf{k}'-\mathbf{k},\eta\tilde{\mathbf{k}}_{\text{tr}}} + \tilde{T}_{\eta\tilde{\mathbf{k}}_{\text{tl}}} \delta_{\mathbf{k}'-\mathbf{k},\eta\tilde{\mathbf{k}}_{\text{tl}}} \right] c_{\text{t},s,\eta}(\mathbf{k}') + h.c., \quad (\text{S55})$$

where

$$\tilde{T}_{\eta\tilde{\mathbf{k}}_{\text{b}}} = \frac{1}{3}t_{\perp} \begin{pmatrix} 1 & 1 \\ 1 & 1 \end{pmatrix}, \quad (\text{S56})$$

$$\tilde{T}_{\eta\tilde{\mathbf{k}}_{\text{tr}}} = \frac{1}{3}t_{\perp} \begin{pmatrix} 1 & e^{-i\eta\frac{2\pi}{3}(1+\sqrt{3}\mathcal{E}_{xx}\mathcal{E}_{xy}+\sqrt{3}\mathcal{E}_{xy}\mathcal{E}_{yy}-\mathcal{E}_{xy}^2-\mathcal{E}_{yy}^2)} \\ e^{i\eta\frac{2\pi}{3}(1+\sqrt{3}\mathcal{E}_{xx}\mathcal{E}_{xy}+\sqrt{3}\mathcal{E}_{xy}\mathcal{E}_{yy}-\mathcal{E}_{xy}^2-\mathcal{E}_{yy}^2)} & 1 \end{pmatrix}, \quad (\text{S57})$$

$$\tilde{T}_{\eta\tilde{\mathbf{k}}_{\text{tl}}} = \frac{1}{3}t_{\perp} \begin{pmatrix} 1 & e^{i\eta\frac{2\pi}{3}(1-\sqrt{3}\mathcal{E}_{xx}\mathcal{E}_{xy}-\sqrt{3}\mathcal{E}_{xy}\mathcal{E}_{yy}-\mathcal{E}_{xy}^2-\mathcal{E}_{yy}^2)} \\ e^{-i\eta\frac{2\pi}{3}(1-\sqrt{3}\mathcal{E}_{xx}\mathcal{E}_{xy}-\sqrt{3}\mathcal{E}_{xy}\mathcal{E}_{yy}-\mathcal{E}_{xy}^2-\mathcal{E}_{yy}^2)} & 1 \end{pmatrix}, \quad (\text{S58})$$

with

$$\begin{aligned} \tilde{\mathbf{k}}_{\text{b}} &= \hat{\mathbf{R}}_{-\frac{\theta}{2}}(1-\mathcal{E}^{\text{T}})\mathbf{K}_{+}-\hat{\mathbf{R}}_{\frac{\theta}{2}}\mathbf{K}_{+} \\ &= -\frac{4\pi}{3\sqrt{3}d}(\mathcal{E}_{xx}\cos\frac{\theta}{2}+\mathcal{E}_{xy}\sin\frac{\theta}{2}, (2-\mathcal{E}_{xx})\sin\frac{\theta}{2}+\mathcal{E}_{xy}\cos\frac{\theta}{2}) \end{aligned} \quad (\text{S59})$$

$$\begin{aligned} \tilde{\mathbf{k}}_{\text{tr}} &= \hat{\mathbf{R}}_{-\frac{\theta}{2}}(1-\mathcal{E}^{\text{T}})(\mathbf{K}_{+}+\mathbf{b}_2)-\hat{\mathbf{R}}_{\frac{\theta}{2}}(\mathbf{K}_{+}+\mathbf{b}_2) \\ &= \frac{2\pi}{9d}((\sqrt{3}\mathcal{E}_{xx}-3\mathcal{E}_{xy})\cos\frac{\theta}{2}+(6+\sqrt{3}\mathcal{E}_{xy}-3\mathcal{E}_{yy})\sin\frac{\theta}{2}, -(3\mathcal{E}_{yy}-\sqrt{3}\mathcal{E}_{xy})\cos\frac{\theta}{2}+(2\sqrt{3}+3\mathcal{E}_{xy}-\sqrt{3}\mathcal{E}_{xx})\sin\frac{\theta}{2}) \end{aligned} \quad (\text{S60})$$

$$\begin{aligned} \tilde{\mathbf{k}}_{\text{tl}} &= \hat{\mathbf{R}}_{-\frac{\theta}{2}}(1-\mathcal{E}^{\text{T}})(\mathbf{K}_{+}-\mathbf{b}_1)-\hat{\mathbf{R}}_{\frac{\theta}{2}}(\mathbf{K}_{+}-\mathbf{b}_1) \\ &= \frac{2\pi}{9d}((\sqrt{3}\mathcal{E}_{xx}+3\mathcal{E}_{xy})\cos\frac{\theta}{2}-(6-\sqrt{3}\mathcal{E}_{xy}-3\mathcal{E}_{xx})\sin\frac{\theta}{2}, (3\mathcal{E}_{yy}+\sqrt{3}\mathcal{E}_{xy})\cos\frac{\theta}{2}+(2\sqrt{3}-3\mathcal{E}_{xy}-\sqrt{3}\mathcal{E}_{xx})\sin\frac{\theta}{2}). \end{aligned} \quad (\text{S61})$$

The interlayer hopping strength is taken as  $t_{\perp} = 0.33\text{eV}$ . As the uniaxial strain deforms the Moire superlattice, the reciprocal primitive lattice vector for the strained Moire superlattice reads

$$\begin{aligned} \tilde{\mathbf{b}}_1^m &= \tilde{\mathbf{k}}_{\text{b}} - \tilde{\mathbf{k}}_{\text{tl}} \\ &= \frac{2\pi}{3d} \left( -(\sqrt{3}\mathcal{E}_{xx}+\mathcal{E}_{xy})\cos\frac{\theta}{2} + (2-\sqrt{3}\mathcal{E}_{xy}-\mathcal{E}_{yy})\sin\frac{\theta}{2}, -(\mathcal{E}_{yy}+\sqrt{3}\mathcal{E}_{xy})\cos\frac{\theta}{2} - (2\sqrt{3}-\mathcal{E}_{xy}-\sqrt{3}\mathcal{E}_{xx})\sin\frac{\theta}{2} \right), \end{aligned} \quad (\text{S62})$$

$$\begin{aligned} \tilde{\mathbf{b}}_2^m &= \tilde{\mathbf{k}}_{\text{tr}} - \tilde{\mathbf{k}}_{\text{b}} \\ &= \frac{2\pi}{3d} \left( (\sqrt{3}\mathcal{E}_{xx}-\mathcal{E}_{xy})\cos\frac{\theta}{2} + (2+\sqrt{3}\mathcal{E}_{xy}-\mathcal{E}_{yy})\sin\frac{\theta}{2}, -(\mathcal{E}_{yy}-\sqrt{3}\mathcal{E}_{xy})\cos\frac{\theta}{2} + (2\sqrt{3}+\mathcal{E}_{xy}-\sqrt{3}\mathcal{E}_{xx})\sin\frac{\theta}{2} \right), \end{aligned} \quad (\text{S63})$$

and the primitive lattice vectors  $\tilde{\mathbf{a}}_1 = (\tilde{a}_{1x}, \tilde{a}_{1y})$ ,  $\tilde{\mathbf{a}}_2 = (\tilde{a}_{2x}, \tilde{a}_{2y})$  are obtained by

$$\begin{pmatrix} \tilde{a}_{1x} & \tilde{a}_{2x} \\ \tilde{a}_{1y} & \tilde{a}_{2y} \end{pmatrix} = \begin{pmatrix} \tilde{b}_{1x}^m & \tilde{b}_{1y}^m \\ \tilde{b}_{2x}^m & \tilde{b}_{2y}^m \end{pmatrix}^{-1} \begin{pmatrix} 2\pi & 0 \\ 0 & 2\pi \end{pmatrix}. \quad (\text{S65})$$

Finally, the Hamiltonian for the twisted bilayer graphene aligned with boron nitride substrate is written as

$$\begin{aligned}\mathcal{H} &= \tilde{\mathcal{H}}_{\text{b}} + \mathcal{H}_{\text{t}} + \tilde{\mathcal{H}}_{\text{int}} \\ &= \sum_{\mathbf{k}, s, \eta} A_{s, \eta}^{\dagger}(\mathbf{k}) h_{\eta}(\mathbf{k}) A_{s, \eta}(\mathbf{k}),\end{aligned}\quad (\text{S66})$$

where  $A_{s, \eta}(\mathbf{k})$  has infinite components representing the series of states  $c_{\text{b}, s, \eta}(\mathbf{k})$ ,  $c_{\text{t}, s, \eta}(\mathbf{k}')$  with  $\mathbf{k} - \mathbf{k}' = \eta \mathbf{k}_{\text{b}}, \eta \mathbf{k}_{\text{tr}}, \eta \mathbf{k}_{\text{tl}}$ . The Hamiltonian matrix  $h_{\eta}(\mathbf{k})$  in the truncated basis  $[a_{\text{b}, s, \eta}(\mathbf{k}), a_{\text{t}, s, \eta}(\mathbf{k} + \eta \mathbf{k}_{\text{b}}), a_{\text{t}, s, \eta}(\mathbf{k} + \eta \mathbf{k}_{\text{tr}}), a_{\text{t}, s, \eta}(\mathbf{k} + \eta \mathbf{k}_{\text{tl}})]^{\text{T}}$  then has the form

$$h_{\eta}(\mathbf{k}) = \begin{pmatrix} h_{\text{b}, \eta}(\mathbf{k}) & \tilde{T}_{\eta \tilde{\mathbf{k}}_{\text{b}}} & \tilde{T}_{\eta \tilde{\mathbf{k}}_{\text{tr}}} & \tilde{T}_{\eta \tilde{\mathbf{k}}_{\text{tl}}} \\ \tilde{T}_{\eta \tilde{\mathbf{k}}_{\text{b}}}^{\dagger} & h_{\text{t}, \eta}(\mathbf{k} + \eta \tilde{\mathbf{k}}_{\text{b}}) & 0 & 0 \\ \tilde{T}_{\eta \tilde{\mathbf{k}}_{\text{tr}}}^{\dagger} & 0 & h_{\text{t}, \eta}(\mathbf{k} + \eta \tilde{\mathbf{k}}_{\text{tr}}) & 0 \\ \tilde{T}_{\eta \tilde{\mathbf{k}}_{\text{tl}}}^{\dagger} & 0 & 0 & h_{\text{t}, \eta}(\mathbf{k} + \eta \tilde{\mathbf{k}}_{\text{tl}}) \end{pmatrix}. \quad (\text{S67})$$

We consider 42 sites in the hexagonal reciprocal lattice so that  $h_{\eta}(\mathbf{k})$  is a  $84 \times 84$  matrix in the calculation for the energy dispersion  $\xi_{\nu, s, \eta, \mathbf{k}}$ . For a specific band with index  $\nu$ , the Bogliubov de-Gennes Hamiltonian in the eigen-band basis  $[\phi_{\nu, \uparrow, \eta, \mathbf{k}}^{\dagger}, \phi_{\nu, \downarrow, \eta, \mathbf{k}}^{\dagger}, \phi_{\nu, \downarrow, -\eta, -\mathbf{k}}, \phi_{\nu, \uparrow, -\eta, -\mathbf{k}}]$  can be written as

$$\begin{pmatrix} H_0(\mathbf{k}) & \hat{\Delta}(\mathbf{k}) \\ \hat{\Delta}^{\dagger}(\mathbf{k}) & -H_0^*(-\mathbf{k}) \end{pmatrix} = \begin{pmatrix} \xi_{\nu, \uparrow, \eta, \mathbf{k}} & 0 & \Delta_{\mathbf{k}} & 0 \\ 0 & \xi_{\nu, \downarrow, \eta, \mathbf{k}} & 0 & -\Delta_{\mathbf{k}} \\ \Delta_{\mathbf{k}} & 0 & \xi_{\nu, \downarrow, -\eta, -\mathbf{k}} & 0 \\ 0 & -\Delta_{\mathbf{k}} & 0 & \xi_{\nu, \uparrow, -\eta, -\mathbf{k}} \end{pmatrix}, \quad (\text{S68})$$

with the singlet pairing  $|\Delta_{\mathbf{k}}| = |\Delta_0 + \lambda \Delta_0 \{\cos(\mathbf{k} \cdot \tilde{\mathbf{a}}_1) + \cos(\mathbf{k} \cdot \tilde{\mathbf{a}}_2) + \cos[\mathbf{k} \cdot (\tilde{\mathbf{a}}_1 - \tilde{\mathbf{a}}_2)]\}|$ .

---

\* wenyuhe@mit.edu

† phlaw@ust.hk

[S1] A. Ramires, and M. Sigrist, Phys. Rev. B **94**, 104501 (2016).

[S2] S. Zhong, J. E. Moore, I. Souza, Phys. Rev. Lett. **116**, 235205 (2015).

[S3] J. Ma, and D. A. Pesin, Phys. Rev. B **92**, 235205 (2015).

[S4] J. M. B. L. Santos, N. M. R. Peres, and A. H. C. Neto, Phys. Rev. Lett. **99**, 256802 (2007).

[S5] J. M. B. L. Santos, N. M. R. Peres, and A. H. C. Neto, Phys. Rev. B **86**, 155449 (2012).

[S6] R. Bistritzer, and A. H. MacDonald, Proc. Natl. Acad. Sci. U. S. A. **108**, 12233 (2011).